



**HAL**  
open science

## **Basal Ti Level in the human placenta and meconium and evidence of a materno-foetal transfer of food-grade TiO<sub>2</sub> nanoparticles in an ex vivo placental perfusion model**

Adèle Guillard, Eric Gaultier, Christel Cartier, Laurent Devoille, Johanna Noireaux, Laurence Chevalier, Mathieu Morin, Flore C. Grandin, Mz Lacroix, Christine Coméra, et al.

### ► To cite this version:

Adèle Guillard, Eric Gaultier, Christel Cartier, Laurent Devoille, Johanna Noireaux, et al.. Basal Ti Level in the human placenta and meconium and evidence of a materno-foetal transfer of food-grade TiO<sub>2</sub> nanoparticles in an ex vivo placental perfusion model. *Particle and Fibre Toxicology*, 2020, 17 (1), 10.1186/s12989-020-00381-z . hal-02945928v1

**HAL Id: hal-02945928**

**<https://hal.inrae.fr/hal-02945928v1>**

Submitted on 9 Oct 2020 (v1), last revised 26 Oct 2020 (v2)

**HAL** is a multi-disciplinary open access archive for the deposit and dissemination of scientific research documents, whether they are published or not. The documents may come from teaching and research institutions in France or abroad, or from public or private research centers.

L'archive ouverte pluridisciplinaire **HAL**, est destinée au dépôt et à la diffusion de documents scientifiques de niveau recherche, publiés ou non, émanant des établissements d'enseignement et de recherche français ou étrangers, des laboratoires publics ou privés.

Dear Author,

Here are the final proofs of your article. Please check the proofs carefully.

Please note that at this stage you should only be checking for errors introduced during the production process. Please pay particular attention to the following when checking the proof:

- Author names. Check that each author name is spelled correctly, and that names appear in the correct order of first name followed by family name. This will ensure that the names will be indexed correctly (for example if the author's name is 'Jane Patel', she will be cited as 'Patel, J.').
- Affiliations. Check that all authors are cited with the correct affiliations, that the author who will receive correspondence has been identified with an asterisk (\*), and that all equal contributors have been identified with a dagger sign (†).
- Ensure that the main text is complete.
- Check that figures, tables and their legends are included and in the correct order.
- Look to see that queries that were raised during copy-editing or typesetting have been resolved.
- Confirm that all web links are correct and working.
- Ensure that special characters and equations are displaying correctly.
- Check that additional or supplementary files can be opened and are correct.

Changes in scientific content cannot be made at this stage unless the request has already been approved. This includes changes to title or authorship, new results, or corrected values.

### **How to return your corrections**

#### *Returning your corrections via online submission:*

- Please provide details of your corrections in the online correction form. Always indicate the line number to which the correction refers.

#### *Returning your corrections via email:*

- Annotate the proof PDF with your corrections.
- Remember to include the journal title, manuscript number, and your name when sending your response via email.

After you have submitted your corrections, you will receive email notification from our production team that your article has been published in the final version. All changes at this stage are final. We will not be able to make any further changes after publication.

Kind regards,

**BioMed Central Production Team**

RESEARCH

Open Access

# Basal Ti level in the human placenta and meconium and evidence of a materno-foetal transfer of food-grade TiO<sub>2</sub> nanoparticles in an ex vivo placental perfusion model

A. Guillard<sup>1</sup>, E. Gaultier<sup>1</sup>, C. Cartier<sup>1</sup>, L. Devoille<sup>2</sup>, J. Noireaux<sup>3</sup>, L. Chevalier<sup>4</sup>, M. Morin<sup>5</sup>, F. Grandin<sup>1</sup>, M. Z. Lacroix<sup>6</sup>, C. Coméra<sup>1</sup>, A. Cazanave<sup>1</sup>, A. de Place<sup>5</sup>, V. Gayrard<sup>1</sup>, V. Bach<sup>7</sup>, K. Chardon<sup>7</sup>, N. Bekhti<sup>8,9</sup>, K. Adel-Patient<sup>8,9</sup>, C. Vayssière<sup>5,10</sup>, P. Fiscaro<sup>3</sup>, N. Feltin<sup>2</sup>, F. de la Farge<sup>1</sup>, N. Picard-Hagen<sup>1</sup>, B. Lamas<sup>1</sup> and E. Houdeau<sup>1\*</sup>

## Abstract

**Background:** Titanium dioxide (TiO<sub>2</sub>) is broadly used in common consumer goods, including as a food additive (E171 in Europe) for colouring and opacifying properties. The E171 additive contains TiO<sub>2</sub> nanoparticles (NPs), part of them being absorbed in the intestine and accumulated in several systemic organs. Exposure to TiO<sub>2</sub>-NPs in rodents during pregnancy resulted in alteration of placental functions and a materno-foetal transfer of NPs, both with toxic effects on the foetus. However, no human data are available for pregnant women exposed to food-grade TiO<sub>2</sub>-NPs and their potential transfer to the foetus. In this study, human placentae collected at term from normal pregnancies and meconium (the first stool of newborns) from unpaired mothers/children were analysed using inductively coupled plasma mass spectrometry (ICP-MS) and scanning transmission electron microscopy (STEM) coupled to energy-dispersive X-ray (EDX) spectroscopy for their titanium (Ti) contents and for analysis of TiO<sub>2</sub> particle deposition, respectively. Using an ex vivo placenta perfusion model, we also assessed the transplacental passage of food-grade TiO<sub>2</sub> particles.

**Results:** By ICP-MS analysis, we evidenced the presence of Ti in all placentae (basal level ranging from 0.01 to 0.48 mg/kg of tissue) and in 50% of the meconium samples (0.02–1.50 mg/kg), suggesting a materno-foetal passage of Ti. STEM-EDX observation of the placental tissues confirmed the presence of TiO<sub>2</sub>-NPs in addition to iron (Fe), tin (Sn), aluminium (Al) and silicon (Si) as mixed or isolated particle deposits. TiO<sub>2</sub> particles, as well as Si, Al, Fe and zinc (Zn) particles were also recovered in the meconium. In placenta perfusion experiments, confocal imaging and SEM-EDX analysis of foetal exudate confirmed a low transfer of food-grade TiO<sub>2</sub> particles to the foetal side, which was barely quantifiable by ICP-MS. Diameter measurements showed that 70 to 100% of the TiO<sub>2</sub> particles recovered in the foetal exudate were nanosized.

(Continued on next page)

\* Correspondence: [eric.houdeau@inrae.fr](mailto:eric.houdeau@inrae.fr)

<sup>1</sup>Toxalim UMR1331 (Research Centre in Food Toxicology), Toulouse University, INRAE, ENVT, INP-Purpan, UPS, Toulouse, France  
Full list of author information is available at the end of the article



© The Author(s). 2020 **Open Access** This article is licensed under a Creative Commons Attribution 4.0 International License, which permits use, sharing, adaptation, distribution and reproduction in any medium or format, as long as you give appropriate credit to the original author(s) and the source, provide a link to the Creative Commons licence, and indicate if changes were made. The images or other third party material in this article are included in the article's Creative Commons licence, unless indicated otherwise in a credit line to the material. If material is not included in the article's Creative Commons licence and your intended use is not permitted by statutory regulation or exceeds the permitted use, you will need to obtain permission directly from the copyright holder. To view a copy of this licence, visit <http://creativecommons.org/licenses/by/4.0/>. The Creative Commons Public Domain Dedication waiver (<http://creativecommons.org/publicdomain/zero/1.0/>) applies to the data made available in this article, unless otherwise stated in a credit line to the data.

(Continued from previous page)

**Conclusions:** Altogether, these results show a materno-foetal transfer of TiO<sub>2</sub> particles during pregnancy, with food-grade TiO<sub>2</sub> as a potential source for foetal exposure to NPs. These data emphasize the need for risk assessment of chronic exposure to TiO<sub>2</sub>-NPs during pregnancy.

**Keywords:** Titanium dioxide, Nanoparticles, Human placenta, E171 food additive, Foetus

## Introduction

Titanium dioxide (TiO<sub>2</sub>) is one of the most commonly produced nanomaterials used for various industrial applications (cosmetics, water and soil treatment, UV filter, medicine, food sector) based on its colouring and opacifying properties as well as its photocatalytic and biocidal activities [1, 2]. Due to these widespread applications, including in food, human exposure to TiO<sub>2</sub> nanoparticles (NPs, at least one dimension < 100 nm) occurs by inhalation, dermal exposure and the oral route. Translocation across biological barriers (lung, skin, intestine) depends on the crystal form (anatase or rutile), coating, size, surface area and aggregate/agglomerate formation [3]. A systemic passage for TiO<sub>2</sub> is documented in human [4–6] and resembles that reported in rodents [7, 8], with accumulation in the liver and spleen of nano- and submicronic particles [9], indicating a low but chronic distribution of TiO<sub>2</sub> particulate matter in the human organism. In vivo studies in rodents exposed to TiO<sub>2</sub> reported toxic effects such as inflammation, impairment of biological barrier functions (intestinal, placental, blood-testis), as well as the promotion of cancer development [7, 10, 11]. Overall, repeated exposure to these particles exhibiting cytotoxic, genotoxic and immunotoxic effects is considered to be an important health issue [12–14]. For the general population, there is accumulating evidence that the main uptake route is ingestion, since TiO<sub>2</sub> is produced at high volumes as a food grade pigment (E171 in EU) incorporated in many foodstuffs as well as in toothpaste, medicines and food supplements. Dietary exposure to TiO<sub>2</sub> ranges from 0.4 to 10.4 mg/kg BW/day [15], depending on the age group and food habits. E171 is a powder consisting of anatase and/or rutile TiO<sub>2</sub>, exhibiting up to 55% NPs by number depending on the commercial supplier [7, 16]. Oral kinetic studies in human volunteers showed that a fraction of food-grade TiO<sub>2</sub> is absorbed and reaches the bloodstream a few hours after ingestion [5]. However, in this context, maternal exposure during pregnancy has not yet been evaluated for risk assessment in humans. Chronic oral intake of TiO<sub>2</sub>-NPs in pregnant women could lead to placental dysfunction and/or transplacental passage, both of which may have deleterious impacts on foetal development [11, 17, 18].

Due to the separation of maternal and foetal circulations, the placenta acts as a barrier to environmental

toxicants [19, 20] and potential pathogens [21] that could be hazardous for the growing foetus. This barrier was nevertheless shown to be poorly effective when exposed to TiO<sub>2</sub>-NPs, at least in mice and rats, with evidence of particle accumulation in the placenta and passage to the foetus [22]. Toxicity data indicate resorption of embryos and foetal growth restriction in mice exposed intravenously to TiO<sub>2</sub>-NPs for two days at mid-pregnancy [17]. Moreover, low doses of TiO<sub>2</sub>-NPs orally administered to dams during the first two gestational weeks were shown to impair placentation and induced dysregulation of vascularization and proliferation, possibly leading to alteration of nutrient and gas exchanges with the foetus [11]. Other studies in rodents exposed through oral route [23–25] or intravenous injection [17, 26] throughout gestation showed a materno-foetal transfer of TiO<sub>2</sub>-NPs and their accumulation in several foetal organs, such as the liver, testis and brain, the latter distribution leading to an impairment of cognitive functions in the offspring. However, all these hazards cannot be directly transposed to humans for risk assessment due to interspecies differences in placentation and structure [27, 28]. Recently, one study reported a significant titanium (Ti) content in the term placenta and in the cord blood in paired mothers-infants, suggesting that a placental transfer of TiO<sub>2</sub> may also exist in humans [29]. Nevertheless, specific data concerning the human placental and meconium content of TiO<sub>2</sub> particles (and particularly NPs) and their transfer are currently lacking. The meconium could be the best matrix to analyse in utero exposure to TiO<sub>2</sub>, as it is the first neonatal stool accumulated during the last 6 months of pregnancy in the foetal intestine. Analysis of meconium, which is naturally excreted within the first two days of life and usually discarded, is non-invasive and considered highly accurate to detect chronic foetal exposure to xenobiotics [30].

In humans, studies on the transplacental passage of inorganic particles have been conducted in vitro on trophoblastic cells and ex vivo using isolated perfused placenta. The size was reported an important contributing factor for particle transfer. Ex vivo, only polystyrene beads up to 240 nm crossed the syncytiotrophoblast that separates the foetal circulation from the maternal blood [31], with low transfer rates and bidirectional passage (i.e., materno-foetal and inversely) [32]. In vitro, 25 and 50 nm silicon (Si) NPs were reported to cross the placental barrier, an observation confirmed ex vivo using

perfused human placenta [33]. These findings suggest the capacity for the nanosized fraction (<100 nm) of food-grade TiO<sub>2</sub> to reach the foetus. To date, in the absence of specific information on food-grade formulations, two studies have examined the capacity of TiO<sub>2</sub>-NP models perfused with different surface charges to cross human placenta. These studies failed to observe a quantifiable increase in Ti levels in the foetal compartment using inductively coupled plasma mass spectrometry (ICP-MS) analysis after 6 h of perfusion, but authors do not exclude the possibility that a low amount of NPs may cross the placental barrier in humans [34, 35], which remains highly challenging to detect. Even in the case of low placental transfer rates, foetal accumulation of insoluble TiO<sub>2</sub>-NPs may occur if the foetus is chronically exposed via its mother to TiO<sub>2</sub> of various environmental origins, including dietary sources.

In this study, we aimed to assess TiO<sub>2</sub> exposure in the human foetus by performing ICP-MS analysis of Ti contents in the human placenta collected at term from pregnancies and in the meconium. These matrices were also analysed with scanning transmission electron microscopy coupled to energy dispersive X-ray (STEM-EDX) analysis to ensure the presence of particles and their chemical nature. Second, by using the ex vivo human placenta perfusion model, we assessed whether TiO<sub>2</sub>-NPs of dietary origin (E171 additive) may cross the placental barrier by combining ICP-MS, confocal microscopy, scanning electron microscopy (SEM) and STEM-EDX for compositional analysis and elemental mapping of the perfused samples in the foetal side and particle distribution into perfused placental tissues.

## Results

### Physico-chemical characteristics of food-grade TiO<sub>2</sub> particles

SEM-EDX analyses showed that E171 had TiO<sub>2</sub> particles with a mean particle size of 104.9 ± 44.9 nm and a particle size distribution ranging from 20 to 440 nm, with 55% of NPs by number (Table 1 and Fig. 1). The specific surface area (SSA) was shown to be 9.6 m<sup>2</sup>/g by BET, and the zeta potential in water suspension was -35.1 ± 3.22 mV (Table 1). DLS analysis showed increased hydrodynamic diameters of the TiO<sub>2</sub> particles in Earle's medium (Table 1), indicating particle agglomeration in the perfusion medium (PM) compared to ultrapure water.

### ICP-MS measurement of total Ti content in the human term placenta and the meconium, and particle analysis by STEM-EDX

As shown in Table 2, Ti was found in all placental samples (*n* = 22), with the total Ti content ranging from 0.01 to 0.48 mg/kg of tissue. Seven women displayed a total placental Ti content above 0.1 mg/kg of tissue, with 2 of them reaching 0.4–0.5 mg/kg of tissue. On TEM tissue sections, particulate matter was observed as isolated primary particles and/or as small aggregates in placental tissues. Chemical elemental mapping using STEM-EDX confirmed the presence of Ti and oxygen (O) onto particle deposits (Fig. 2a), often appearing as elongated crystal forms associated with aluminium (Al) and Si trace elements, and most of the analysed TiO<sub>2</sub> particles were below 100 nm in diameter (Fig. 2a). Among the 34 particles analysed by EDX, Si-, tin (Sn)-, Al-, iron (Fe)- and zinc (Zn)-containing particles were frequently found in addition to TiO<sub>2</sub> (Fig. S1). Size measurements of all particles (i.e., whatever their chemical nature) recovered during the TEM analysis showed that 32 of 34 particles exhibited diameters ranging from 10 to 225 nm, 16 of them (i.e., 50%) being below 100 nm (Fig. S2), and two large agglomerates of 320 and 380 nm (Fig. S2).

In the meconium (Table 2), Ti was detected by ICP-MS in 50% of samples (9 of 18), ranging from 0.02 to 1.50 mg/kg of material. In most of these samples (*n* = 8), the Ti levels were above 0.1 mg/kg of meconium (Table 2). TEM-EDX analysis of two representative meconium samples confirmed the presence of Ti and O elements in the particulate deposits (Fig. 2b). In addition, clustered elements of mainly Si, Al, Fe and Zn were observed as particulate matter (Fig. S3). Overall, size analysis of all particles indicated a diameter ranging from 5 to 194 nm (*n* = 33 particles), and 26 of them (i.e., 82%) were in the nanorange.

### Transfer profile of food-grade TiO<sub>2</sub> particles across the human placenta ex vivo

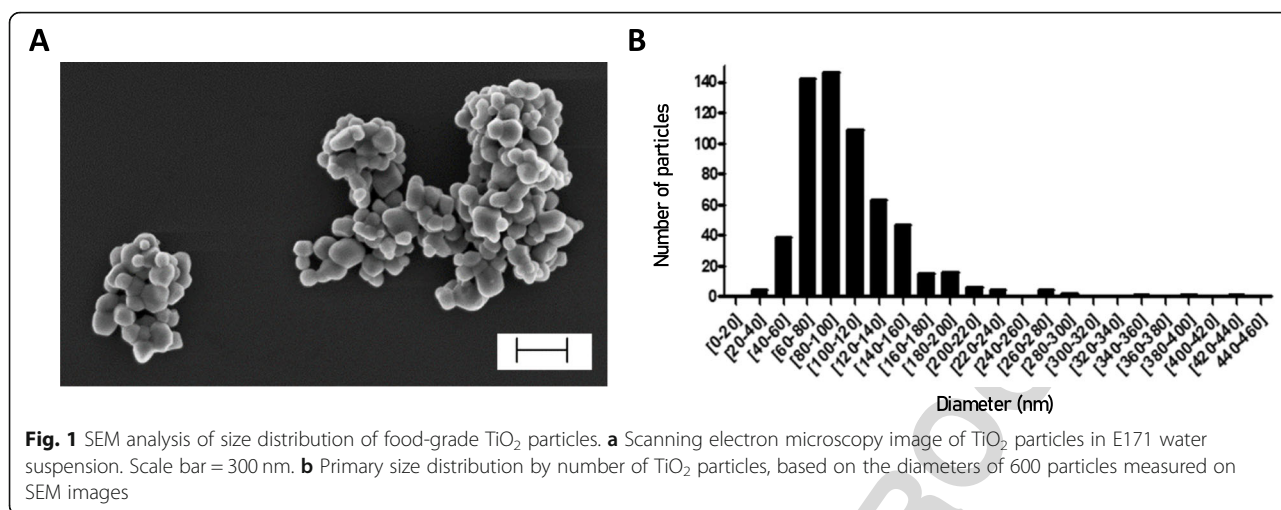
A total of 7 placentae were validated based on antipyrine passage during ex vivo perfusion in an open circulating system with PM alone and E171 suspension. There was no difference in permeability (i.e., antipyrine transfer rate) between placentae collected after caesarean section or vaginal delivery (Fig. S4). After the perfusion of placentae with food-grade TiO<sub>2</sub> (E171), Ti was detected by ICP-MS in most foetal exudates (0.41 to 3.46 ng Ti/mL), but 92% were in the range of the blank level (0.33 to

F1 T1

**Table 1** Physico-chemical characteristics of E171

	Mean particle size (nm)	% of NPs	SSA (m <sup>2</sup> /g)	Ultrapure water (pH = 8.92)			Perfusion medium (pH = 7.40)		
				Zeta potential (mV)	H. diam. (nm)	Pdl	Zeta potential (mV)	H. diam. (nm)	Pdl
	104.9 ± 44.9	55	9.6	-35.1 ± 3.22	303.27 ± 134.27	0.223	-12.3 ± 0.00	383.3 ± 163.6	0.363

All data are presented as mean ± SD. SSA specific surface area, H. diam. hydrodynamic diameter, Pdl polydispersity index



Q6]f1.1  
f1.2  
f1.3  
f1.4

230 1.92 ng Ti/mL) (Table S1). To assess whether a transfer  
231 occurred for TiO<sub>2</sub> particles, we examined the exudate  
232 samples collected every 5 min on the foetal side by con-  
233 focal microscopy to detect laser-diffracting (TiO<sub>2</sub>-like)  
234 particles, as shown in Fig. S5. An average blank value of  
235 1.05 ± 0.32 laser-diffracting spots per microscopic field  
236 was calculated from 4 independent experiments with  
237 PM free of E171, and then subtracted from each time  
238 point in each placenta perfused with the E171 suspen-  
239 sion. As shown in Fig. 3, the placental translocation of  
240 laser-diffracting TiO<sub>2</sub> particles increased from 10 min of  
241 E171 perfusion, reached a plateau at 20–30 min, and  
242 then decreased until the end of the perfusion.

**F3** 243 **SEM-EDX analysis of perfused particles recovered in the**  
244 **foetal exudate**

245 Based on the above reported particle transfer profile  
246 with confocal imaging, pooled liquid fractions in the  
247 foetal side corresponding to the 20–30 min period of  
248 perfusion with the E171 suspension (see Fig. 3) were  
249 subjected to SEM-EDX analysis. After sample purifica-  
250 tion, SEM-EDX scanning showed the presence of many  
251 TiO<sub>2</sub> particles appearing as isolated particles or aggre-  
252 gates trapped in the matrix of the dried PM (Fig. 4). Fur-  
253 thermore, Al and Fe elements were also found in some  
254 particulate deposits, associated or not with Ti (Fig. S6).  
255 The current detection method by SEM-EDX did not  
256 provide quantitative information on the total number of  
257 TiO<sub>2</sub> particles recovered in the foetal circuit over the  
258 20–30 min of E171 perfusion but allowed us to evaluate  
259 the size distribution of the particles crossing the placenta  
260 during this period. As a result, a total of 300 TiO<sub>2</sub> parti-  
261 cles sampled and purified from the foetal side were mea-  
262 sured by taking the smallest dimension observed for  
263 each TiO<sub>2</sub>-positive particle in the recovered agglomer-  
264 ates (Fig. S7), and the results compared to the TiO<sub>2</sub> par-  
265 ticle size distribution in the PM with E171 added from

the maternal reservoir (Fig. 5). Except for 3 particles, 266 **F5**  
267 TiO<sub>2</sub> particles recovered in the foetal side exhibited a  
268 diameter < 200 nm, with 70 and 100% of NPs in two per-  
269 fusion experiments (Fig. 5).

**STEM-EDX analyses of TiO<sub>2</sub> particles in the perfused** 270  
**placental tissues** 271

In placental tissue, (S)TEM-EDX was used to investigate 272  
the distribution of TiO<sub>2</sub> particles into the perfused coty- 273  
ledon. As illustrated in Fig. 6, enriched tissue areas with 274 **F6**  
275 Ti + O showed isolated round shaped particles or small  
276 aggregates of TiO<sub>2</sub>, typical of the food-grade batch used  
277 in this study. TiO<sub>2</sub> particles from the E171 suspension  
278 were recovered in the syncytiotrophoblast microvilli (Fig.  
279 6a and S8D) and had translocated in deeper areas of the  
280 placental chorionic mesenchyme surrounding foetal ves-  
281 sels (Fig. 6b and S8D). As shown in Fig. S8, size mea-  
282 surement of the 33 TiO<sub>2</sub> (i.e., EDX-characterized)  
283 particles translocated into placental tissues showed 26  
284 particles with a diameter below 250 nm, and 17 of them  
285 in the nanorange.

**Discussion** 286

The effects of prenatal exposure to xenobiotics (poten- 287  
tially toxic) on birth outcomes and child development 288  
are an area of concern for public health [36], which have 289  
been extended to NPs of anthropogenic origin, including 290  
TiO<sub>2</sub>-NPs. For pregnant women, a recent opinion by the 291  
French High Council for Public Health [37] indicated that 292  
the risk of a transfer of TiO<sub>2</sub>-NPs to the foetus and 293  
the health consequences for the newborn have not been 294  
documented despite animal studies showing harmful ef- 295  
fects [22], with TiO<sub>2</sub>-NPs recovered in foetal organs 296  
such as the brain, liver and testis [17, 23, 26]. A recent 297  
study in humans analysed the Ti content in maternal 298  
and cord blood and suggested a high placental transfer 299  
efficiency of Ti [38]. Titanium was also evidenced in the 300

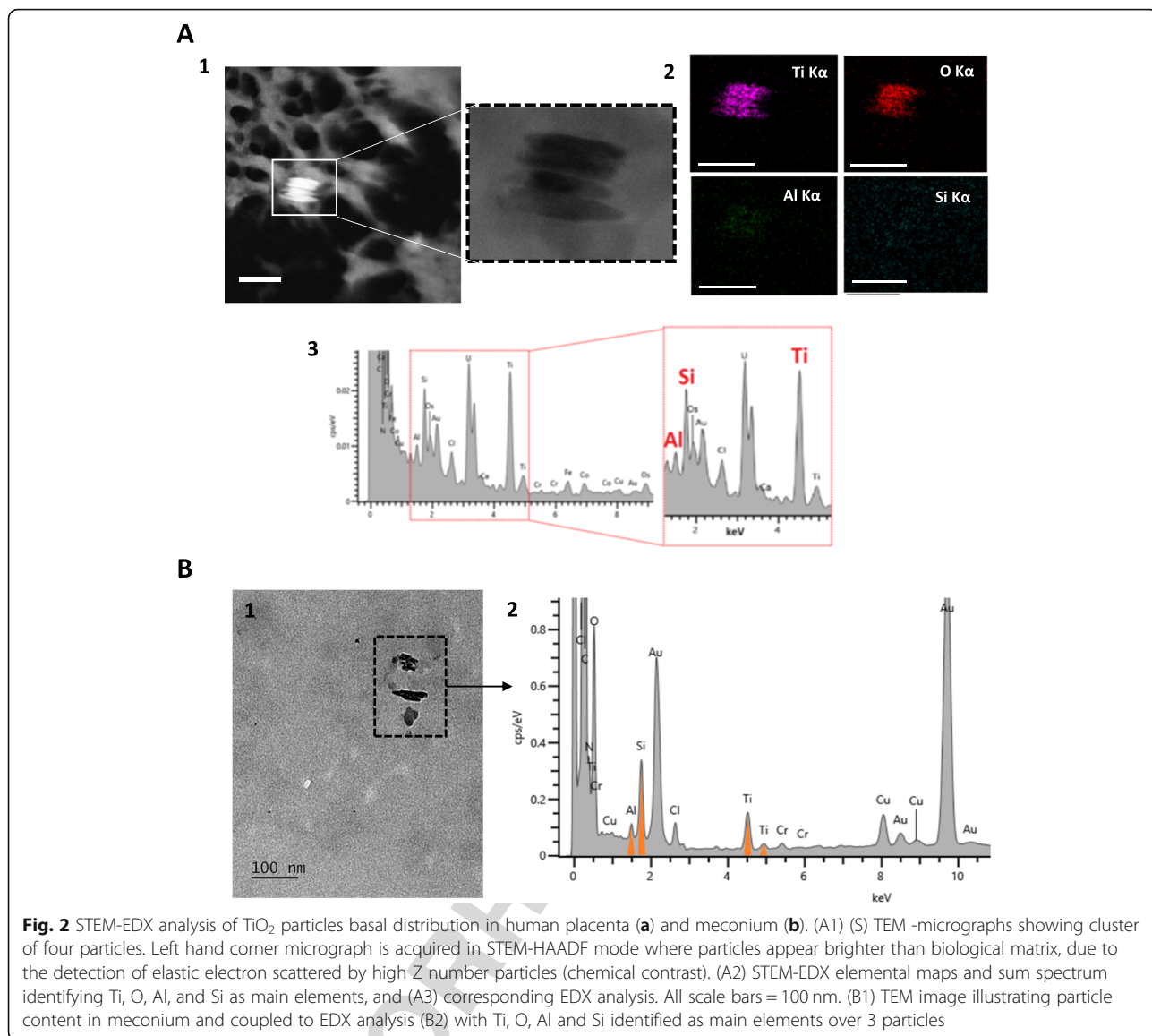
t2.1 **Table 2** ICP-MS analysis of basal Ti content in human term  
t2.2 placenta and meconium (unpaired samples)

t2.3	Total Ti (mg/kg)	
	Placenta (n = 22)	Meconium (n = 18)
t2.4		
t2.5	1	0.04
t2.6	2	0.02
t2.7	3	0.01
t2.8	4	0.05
t2.9	5	0.20
t2.10		
t2.11	6	0.15
t2.12	7	0.03
t2.13	8	0.17
t2.14	9	0.11
t2.15	10	0.05
t2.16	11	0.03
t2.17	12	0.01
t2.18	13	0.16
t2.19	14	0.02
t2.20	15	0.47
t2.21	16	0.06
t2.22	17	0.09
t2.23	18	0.04
t2.24	19	0.08
t2.25	20	0.48
t2.26	21	0.01
t2.27	22	0.03
t2.28	n > LOQ	100%
t2.29	average	0.10
t2.30	SD	0.13
t2.31	min	0.01
t2.32	max	0.48
t2.33	median	0.05
t2.34	1st quartile	0.03
t2.35	3rd quartile	0.14
t2.36	Samples were obtained from unpaired mother-infants. All concentrations are	
t2.37	corrected for total blank signals. *Weighted mean for 3 analyses. LOQ = 0.01	
t2.38	mg/kg for meconium and 0.003 mg/kg for placenta. Typical relative	
t2.39	measurement uncertainties were 6.5% (k = 1) for meconium, and 8% (k = 1)	
t2.40	for placenta	

Ti content in these biological matrices together with the morphology, size and chemical characterization of the particles identified in the placental tissue sections and in the meconium preparations for electron microscopy. We report that all collected placentae from term pregnancies had a quantifiable amount of Ti, with an average level of 0.10 mg/kg of tissue, which is consistent with the findings of Li et al. [29] (0.2 mg/kg) and close to the Ti concentrations under particulate form in the human liver and spleen, as previously measured by single particle (sp) ICP-HRMS in organs recovered post-mortem [9]. Furthermore, seven placentae exhibited Ti contents between 0.1 and 0.5 mg/kg of tissue, these amounts being comparable to the maximum Ti levels reported in the human spleen [9], suggesting a high capacity of the placenta to accumulate Ti(O<sub>2</sub>) from the maternal blood. TEM imaging coupled to EDX analysis showed the presence of isolated and clustered TiO<sub>2</sub> particles; most of the constitutive particles were spherical and assumed to have an anatase crystal structure, while others consisted of elongated TiO<sub>2</sub> particles typical of the rutile forms. The rutile and anatase forms of TiO<sub>2</sub> are authorized in the formulations of the E171 food additive in the EU (EC Regulation n°231/2012), while rutile is also commonly used in sunscreens and cosmetics such as day creams and loose and pressed powders [40, 41], with possible inhalation and/or absorption through the skin, although very few studies have revealed dermal penetration through intact skin [3]. Furthermore, TiO<sub>2</sub> is used as an opacifying agent in indoor paints with particles released into domestic air with dust and pulmonary exposure [42–44]. However, all these different routes of exposure cannot be discriminated on the sole base of the crystal forms recovered in the tissue due to their different usages both in the environment and in consumer products. Furthermore, we consistently identified particle deposits of Al, Si, Fe, Sn and Zn in the term placentae. These accumulated particles may originate from dietary intake [45] and pharmaceutical products [5] along with other sources such as air pollution in an urban environment [46–48]. With the example of tin, our data showing deposition as particles in the human placenta are consistent with the exposure profiles to Sn measured in the maternal blood and the tin accumulation in the placenta as reported by ICP-MS measurements [49], which requires further research regarding placental transfer.

For meconium, 50 % of the samples had a quantifiable amount of Ti (range 0.02–1.50 mg/kg), with some of them exhibiting Ti contents well above those recovered in the placenta. Meconium reflects a long window of exposure and is considered a relevant matrix in toxicology screening for detecting foetal exposure to various xenobiotics, such as airway pollutants, heavy metals,

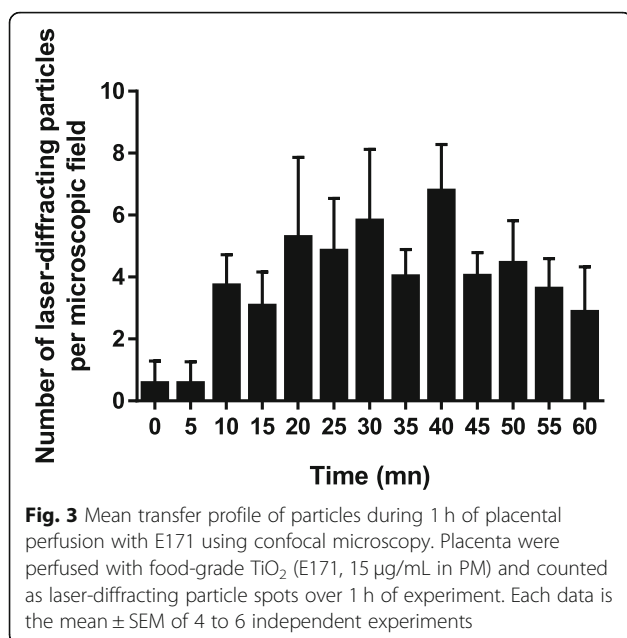
301 amniotic fluid, even if the prevalence of pregnant  
302 women exhibiting amniotic Ti load is quite low [39].  
303 However, whether Ti signal originated from (nano) particulate matter was not specified and, to date, no analytical data exist on the potential accumulation of TiO<sub>2</sub> particles in the human placenta and the meconium, the latter being used herein as a biomarker of prenatal exposure of the newborn to TiO<sub>2</sub> from the mother. In this study, a combination of two analytic methods with ICP-MS and STEM-EDX allowed us to determine the total



f2.1  
f2.2  
f2.3  
f2.4  
f2.5  
f2.6

365 pesticides or pharmaceuticals, with which pregnant  
366 women are in contact [30, 50]. These chemicals can mi-  
367 grate into the foetus directly from the placental interface  
368 through the cord blood or come from the amniotic fluid  
369 of which formation partly results from transudation of  
370 maternal fluids together with secretions of the amnion  
371 epithelium [51]. Because meconium matrix contains am-  
372 niotic fluid mixed with foetal urines, all being continu-  
373 ously swallowed (as well as inhaled) by the foetus during  
374 pregnancy, and reabsorbed by the foetal intestine [51],  
375 such matrix may reflect global foetal body exposure to  
376 TiO<sub>2</sub>. From the current ICP-MS analysis, the high vari-  
377 ability of Ti content among the meconium samples, as  
378 shown in placenta, suggests inter-individual differences  
379 in mothers' exposure to TiO<sub>2</sub> and/or in basal permeabil-  
380 ity of biological barriers to TiO<sub>2</sub> that remain unexplored.

381 Given the maternal origin of xenobiotics in meconium  
382 [30], it is assumed that foetal exposure to TiO<sub>2</sub> directly  
383 relies on the mother's use of TiO<sub>2</sub>-containing products  
384 and/or TiO<sub>2</sub> emission in her environment, which may  
385 have multiple origins on a household basis, as noted  
386 above. In our study, further EDX analysis confirmed  
387 TiO<sub>2</sub> particle deposition in the meconium. Furthermore,  
388 all the recovered TiO<sub>2</sub> particles were nanosized and  
389 often exhibited morphology resembling that of elongated  
390 TiO<sub>2</sub> (putative rutile) structures, as observed in the  
391 placental tissues. In addition, Fe particles and particulates  
392 deposits with Al and Si were found in the meconium as  
393 in the placenta. Notably, materno-foetal translocation  
394 of Si-NPs has been demonstrated in vitro in the placen-  
395 tal BeWo cell line [33], which represents the rate-  
396 limiting barrier for maternal-foetal exchange, as well as



f3.1  
f3.2  
f3.3  
f3.4  
f3.5  
f3.6

basal Ti blood level in humans (10 µg/L) [4, 5] in order to optimize particle detection under a short time of perfusion (i.e., maximum 6 h) and given the short viability of the placenta ex vivo in a non-recirculating system. A high TiO<sub>2</sub> concentration in perfusion medium could rapidly lead to clogging of the intervillous space on the maternal side, limiting particle recovery on the foetal side. Indeed, in the study of Wick et al. (2010) using 25 µg/mL PS beads for a 6 h perfusion, nanosized beads were reported to cross the placental barrier only during the first hour, with no subsequent transfer when the PS beads were de novo added after 3 h in the maternal compartment. The authors suggested that the high dose of particles in the intervillous spaces created an agglomeration close to the placental villus on the maternal side, preventing the transfer of beads to the foetal compartment after a certain time [31]. These results suggested that a similar situation for TiO<sub>2</sub> particles could explain the low Ti levels on the foetal side, as reported in the above perfusion studies [34, 35]. In our study, we focused on a one-hour perfusion to limit the risk of placental obstruction by TiO<sub>2</sub> particles from the perfusion medium with E171.

To avoid uncertainties in our study, we used confocal microscopy for particle visualization in the foetal effluent (i.e., appearing as laser-diffracting metal particles in the exudate) and SEM-EDX analysis to ascertain their chemical nature as TiO<sub>2</sub> particulate matter. Based on the confocal transfer profile, a progressive increase of the TiO<sub>2</sub> particles was recovered in the foetal side as soon as 10 min after the E171 suspension was added in the maternal compartment. Interestingly, a rapid passage was also reported for gold (Au) NPs (20 nm) across the rat placenta via ex vivo perfusion, i.e., within 20 min following material infusion [57]. In our study, given the poorly quantifiable level of Ti by ICP-MS in the foetal effluent following E171 perfusion, it is assumed that the mean transfer rate of the TiO<sub>2</sub> particles over time is very low. However, given that our experiment was conducted for only 1 h, the overall transfer of particles during the whole duration of pregnancy could account for a non-negligible accumulation of TiO<sub>2</sub> (nano) particles in the foetal body. This assumption is well supported by our above demonstration of the presence of Ti in 50% of the meconium samples collected for this study. Furthermore, we showed that a large majority of the TiO<sub>2</sub> particles found in the foetal exudate after E171 perfusion was in the nanorange. Because the size distribution of TiO<sub>2</sub> particles recovered into tissues of a perfused cotyledon showed 50% composed of TiO<sub>2</sub> nanofoms, this suggested that the fraction of larger TiO<sub>2</sub> particles remained mostly trapped into the placental tissues and did not reach the foetal compartment. Both these findings indicate that the placenta cannot be considered as an

ex vivo in perfused human placenta [33] and in vivo in mice [52]. For Al and Si particle deposits, as noted above, both elements are ubiquitous in the environment and diet [45, 53, 54]. Finally, for TiO<sub>2</sub>, because the present study was not conducted on mother-child pairs, it is not possible to relate the Ti levels measured in the meconium to the amount found in the placenta. Nonetheless, altogether, the current findings provide evidence of a materno-foetal passage of TiO<sub>2</sub> nanoparticles in humans.

To confirm this passage, we conducted a study using the ex vivo human placenta perfusion model considered the gold standard for studying human materno-foetal transfer of xenobiotics [55], including nanoparticles [31, 32]. We focused on E171 food additives due to recent risk assessment studies highlighting oral ingestion as the major TiO<sub>2</sub> route of exposure in the general population [9, 56]. This conclusion was based on the substantial daily ingestion of food-grade TiO<sub>2</sub> used as an E171 additive (up to several milligrams per kilogram of BW per day [15]) in the absence of an acceptable daily intake, and on toxicokinetic information for accumulation in organs and clearance from tissues [56]. We first showed poorly detectable Ti signals in the foetal exudate, suggesting a passage of particles too low to be distinguished from the blank levels after 1 h of E171 perfusion. Similar observations have been reported by other groups after 6 h of perfusion with TiO<sub>2</sub>-NPs models, with Ti signals in the range of the background levels of the control perfusion medium [34, 35], as herein reported. In these studies, including the present, the TiO<sub>2</sub> concentration used for perfusion (10 to 25 µg/mL for toxicokinetic purposes) was approximately 1000 times higher than the

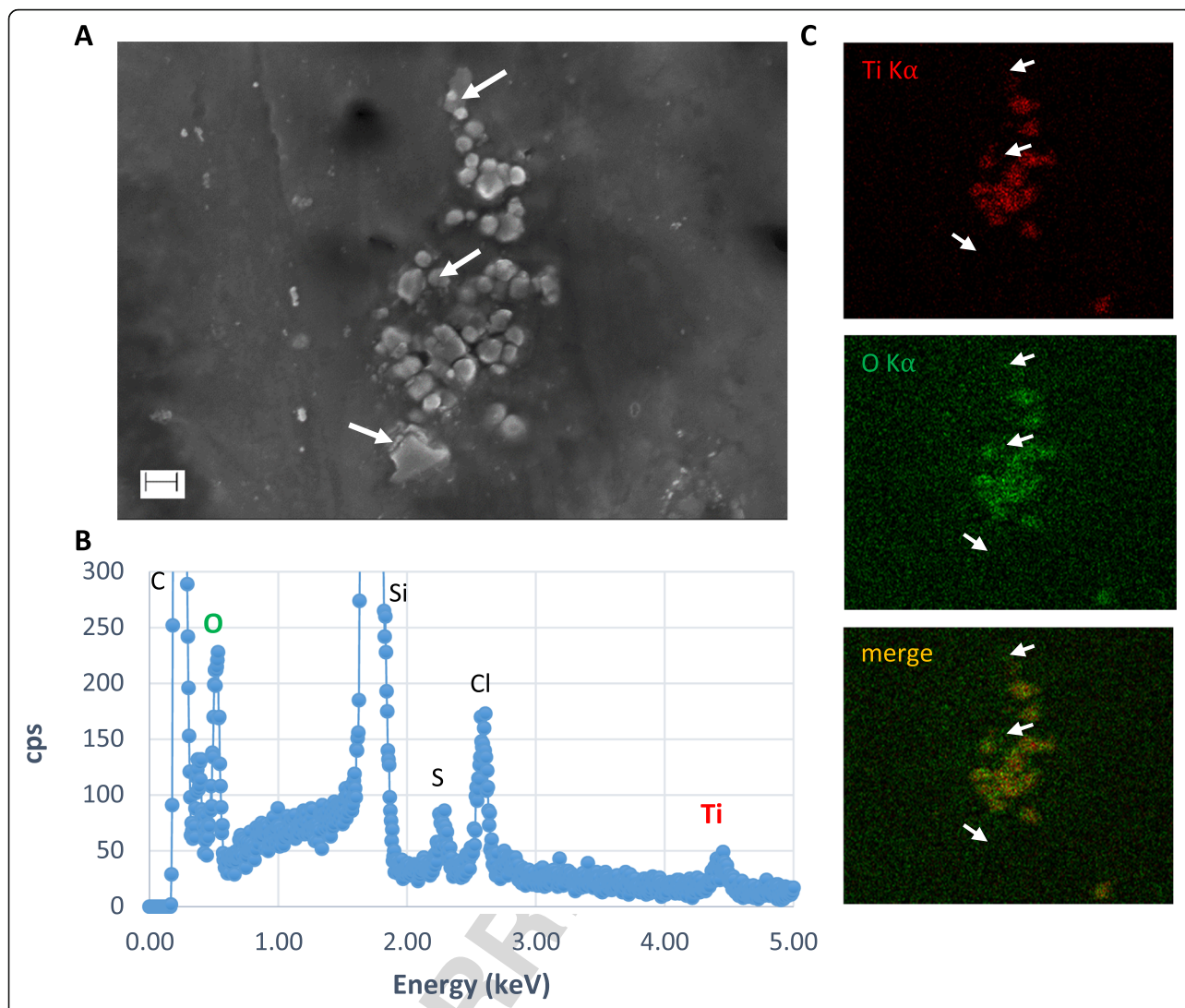


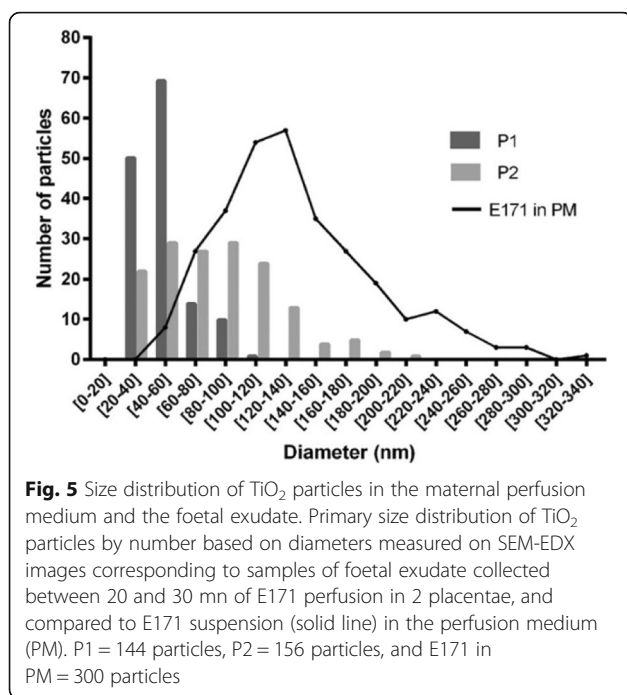
**Fig. 4** Analysis of TiO<sub>2</sub> particles by SEM-EDX in foetal exudate. **a** SEM images of particles agglomerated in the dried PM after sample preparation of foetal exudate taken up from the 20–30 min period of perfusion. **b** Corresponding EDX analyses of particles into agglomerates showing the presence of C, Cl, S, Ti and O (Si signal from SEM wafer). **c** SEM-EDX cartography of particles showing Ti (red) and O (green) elements, and corresponding merge image. White arrows indicate examples of particles negative for Ti and O in this preparation. Scale bar = 200 nm

f4.1  
f4.2  
f4.3  
f4.4  
f4.5

484 absolute barrier preventing the passage of TiO<sub>2</sub> NPs  
 485 from the maternal blood, as previously reported using  
 486 PS beads or Au-NPs with similar perfusion ap-  
 487 proaches [31, 58]. To date, the mechanisms for NP  
 488 translocation are still unknown, but the main hypoth-  
 489 esis for NP transport involves transtrophoblastic  
 490 channels and/or endocytotic mechanisms across the  
 491 placental barrier [32, 58, 59].  
 492 From a risk perspective, animal studies raised concerns  
 493 about NPs entering the foetus in rodents exposed  
 494 through inhalation or the transcutaneous or oral route.  
 495 A large variety of effects on developmental processes  
 496 have been reported for TiO<sub>2</sub>-NPs, particularly on brain  
 497 functions due to translocation through the foetal blood-  
 498 brain barrier, with consequences on behaviour [22]. In

addition, because immunotoxic and antibacterial proper-  
 ties have been reported for TiO<sub>2</sub> (nano) particles, includ-  
 ing the food-grade form [7, 60–63], their accumulation  
 in the foetal gut through the meconium, as shown  
 herein, could affect the primary colonization of the in-  
 testine by the microbiota at birth as well as the matur-  
 ation of the intestinal immune system, two perinatal  
 events of which dysfunctions have long-term health con-  
 sequences, as recently reviewed [64]. Accumulation in  
 the placenta may also lead to placental dysfunction (e.g.,  
 dysregulation of vascularization, inhibition of cell prolif-  
 eration, induction of apoptosis) and subsequent foetal  
 growth restriction [11]. In addition to the findings in  
 these rodent studies, TiO<sub>2</sub>-NPs can trigger autophagy  
 and mitochondrial dysfunction in vitro in human

499  
500  
501  
502  
503  
504  
505  
506  
507  
508  
509  
510  
511  
512  
513



f5.1  
f5.2  
f5.3  
f5.4  
f5.5  
f5.6  
f5.7  
f5.8  
f5.9

need to assess the risk of TiO<sub>2</sub>-NP exposure in pregnant women and warrant specific attention for oral exposure to the nanosized fraction of the E171 food additive.

## Methods

### Particle characterization and preparation

The E171 food additive was purchased as powder from the website of a French commercial supplier of food colouring agents. These food-grade TiO<sub>2</sub> particles were prepared following the generic Nanogenotox dispersion protocol as previously described [7]. The E171 stock suspension (25.6 mg/mL) was sonicated in an ice bath for 16 min at 30% amplitude (VCX 750-230 V, Sonics Materials) to obtain a stable dispersion of TiO<sub>2</sub> particles and then stocked at 4 °C during 15 days maximum before use. Dynamic light scattering (DLS, ZetaSizer nano ZS; Malvern Instruments Ltd.) measurements were performed on TiO<sub>2</sub> particles in ultrapure water (pH = 8.92) and perfusion medium (PM = Earle + 2% BSA, pH 7.4). Five μL of E171 stock suspension were diluted in 3 mL of PM and the hydrodynamic diameter (Z-average), polydispersity index and zeta potential of the TiO<sub>2</sub> particles were measured. Particle diameters were measured by scanning electron microscopy (SEM, *n* = 600 particles) and are expressed as the percentage of NPs by number. The specific surface area (SSA) of the particles was assessed according to the Brunauer, Emmet and Teller method (BET).

### Human placenta and meconium collection

The study was conducted in accordance with the Declaration of Helsinki and its later amendments. Placentae and meconium were collected from different sites and thus were not from mother-infant pairs. Term placentae were collected from 22 uncomplicated pregnancies in the CHU Paule de Viguiet (Toulouse, France; Institutional approval (DC-2013-1950). Signed informed consent was obtained from all the mothers. Meconium samples (< 48 h post-partum) were collected in the maternity ward of Sainte-Thérèse Clinic (Paris, France), under an internal agreement of the scientific committee (*n* = 11), or from volunteer parents (*n* = 7). Informed signed consents were obtained from all parents. Meconium collection is non-invasive as it is directly recovered by scraping stained diaper with a sterile disposable spatula, taking care not touching nappy surface.

For basal Ti level determination in all placentae and meconium, a biopsy from one cotyledon per placenta and all meconium samples were weighed and stored at -80 °C before analysis. Samples from 2 placentae and 2 meconium were also prepared for STEM-EDX analysis.

For ex vivo perfusion experiments, after a visual examination of organ integrity, 15 placentae (623 ± 186 g)

514 trophoblast cells [65, 66], and further impair the cell mi-  
515 gration [67] that is needed for trophoblastic invasion in  
516 the uterine wall, permitting embryo implantation. There-  
517 fore, additional studies are needed to quantify and fur-  
518 ther characterize the human foetal exposure to TiO<sub>2</sub>-  
519 NPs shown in our study, together with studies in ani-  
520 mals chronically exposed to TiO<sub>2</sub> during pregnancy, in-  
521 cluding from the oral route, to determine the potential  
522 hazards for foetal development and newborn health.

## 523 Conclusion

524 By combining different methods for particle detection,  
525 element composition and size analysis together with Ti  
526 quantification, the present study highlighted the passage  
527 of TiO<sub>2</sub> particles across the human placenta with poten-  
528 tial local accumulation during pregnancy depending on  
529 individuals. Even if the placental transfer could not be  
530 quantified, a translocation to the foetal body seems to  
531 exist, as reflected by the Ti content and TiO<sub>2</sub> particle  
532 deposits in meconium samples, mainly of nanosized  
533 forms, that suggest prenatal TiO<sub>2</sub> exposure from various  
534 sources. We further demonstrated TiO<sub>2</sub> particle transfer  
535 through isolated human placenta perfused with food-  
536 grade TiO<sub>2</sub> from the E171 additive, concluding that the  
537 human placental barrier is unable to completely prevent  
538 the passage of TiO<sub>2</sub>-NPs from dietary sources and pro-  
539 tect the foetus. Finally, given the current study showing  
540 ex vivo a materno-foetal passage of nanosized TiO<sub>2</sub> par-  
541 ticles in humans, together with quantitative data from  
542 different cohorts showing placental and meconium Ti  
543 load at term of pregnancy, our findings emphasize the

Q5

547

548

549

550

551

552

553

554

555

556

557

558

559

560

561

562

563

564

565

566

567

568

569

570

571

572

573

574

575

576

577

578

579

580

581

582

583

584

585

586

587

588

589

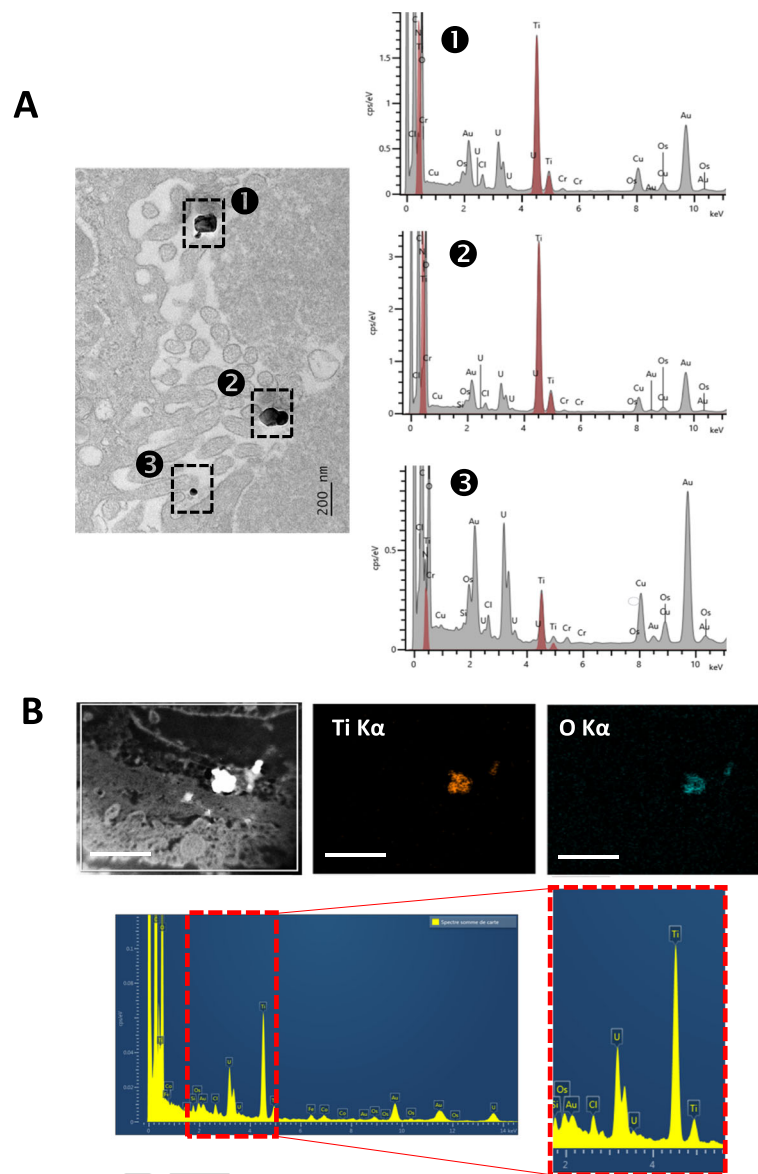
590

591

592

593

594



f6.1 **Fig. 6** Tissue distribution of  $\text{TiO}_2$  particles in the E171 perfused placenta. **a** TEM-Bright-Field micrographs coupled to EDX analysis showing food-  
 f6.2 grade  $\text{TiO}_2$  particles into the syncytiotrophoblast microvilli. **b** Chemical characterization of  $\text{TiO}_2$  particles by STEM-EDX mapping based on STEM-  
 f6.3 HAADF micrographs for particle detection, and elemental maps and sum spectrum. Scale bars in (B) = 1  $\mu\text{m}$   
 f6.4

595 collected after caesarean section ( $n = 8$ ) or normal vagi-  
 596 nal delivery ( $n = 7$ ) were used.

#### 597 Ex vivo placental perfusion model

598 The placentae were transported in a thermostatically  
 599 controlled container ( $37^\circ\text{C}$ ) and prepared for perfusion  
 600 within 1 h of delivery in an open double circuit system  
 601 as previously described [68]. Briefly, an intact peripheral  
 602 cotyledon was chosen, and the truncal branch of the  
 603 chorionic artery supplying the cotyledon and its associ-  
 604 ated vein were catheterized (Microtube Tygon S54-HL  
 605 1.02\*1.78 mm, Courbevoie, France). The perfusion

medium (PM) was Earle's medium (Euromedex, Souffel  
 606 Weyersheim, France) supplemented with 2 g/L of BSA  
 607 (Fraction V, PAA Laboratories, Vélizy-Villacoublay,  
 608 France), and the foetal flow rate was established at 6  
 609 mL/min. After a few minutes, the perfused cotyledon  
 610 progressively whitened, allowing its isolation and was  
 611 placed into a thermostatically controlled glass receptacle  
 612 maintained at  $37^\circ\text{C}$ , with maternal side facing upwards.  
 613 Two hypodermic cannulas were used to perfuse the ma-  
 614 ternal side of the placenta with a flow rate established at  
 615 12 mL/min. Each placenta was perfused for 30 min with  
 616 PM alone to flush the blood out of the maternal and  
 617

618 foetal circulation and then for 1 h with ( $n = 13$ ) or with-  
619 out ( $n = 2$ ) PM with food-grade (E171)  $\text{TiO}_2$  (15  $\mu\text{g}/\text{mL}$ ).  
620 To ensure proper dispersion, the E171 stock suspension  
621 was vigorously agitated using a vortex before addition in  
622 the maternal circulation. The perfusion medium was  
623 under constant agitation for oxygenation, allowing the  
624 homogeneous dispersion of  $\text{TiO}_2$  particles.

625 During the whole perfusion time (90 min), the foetal  
626 and maternal pH values were continuously adjusted  
627 throughout the experiments to  $7.27 \pm 0.05$  and  $7.41 \pm$   
628  $0.01$  (mean  $\pm$  SD), respectively, and the temperature and  
629 flow rates were checked. Antipyrine (Sigma-Aldrich), a  
630 reference control substance for passive diffusion and  
631 barrier integrity, was added to the maternal reservoir  
632 (20  $\mu\text{g}/\text{mL}$ ) at the beginning of the perfusion ( $t_0$ ), and  
633 antipyrine concentrations were measured in foetal exu-  
634 dates collected every 15 min by high performance liquid  
635 chromatography coupled with UV detection. All placen-  
636 tae with a maternal to foetal transfer of antipyrine lower  
637 than 20% were excluded from the study.

638 For assessment of the materno-foetal transfer of  $\text{TiO}_2$   
639 particles, repeated samples (2 mL each) from the foetal  
640 flow through were collected every 5 min before and after  
641 E171 addition on the maternal side and stored at  $4^\circ\text{C}$   
642 after the addition of fungizone (3.5  $\mu\text{L}/\text{mL}$ ) and penicil-  
643 lin + streptomycin (10  $\mu\text{L}/\text{mL}$ ) to prevent from bacterial  
644 growth. These samples were used for confocal micros-  
645 copy detection of laser-reflecting particulate matter that  
646 reached the foetal side. In addition, pools of foetal exu-  
647 date ( $\approx 50$  mL) were collected by 10- or 15-min periods  
648 over the whole perfusion time and then stored at  $-20^\circ\text{C}$   
649 for subsequent ICP-MS analysis of the Ti concentration  
650 and SEM-EDX detection of the  $\text{TiO}_2$  particles.

651 At the end of the experiment, the perfused cotyledon  
652 was washed for 20 min with PM only to flush out  $\text{TiO}_2$   
653 particles that did not penetrate the tissue. Tissue sam-  
654 ples were collected close to the perfusion cannula and  
655 taken along the materno-foetal axis as representative  
656 areas for particle diffusion from the maternal side to the  
657 foetal circuit, while adjacent non-perfused cotyledons  
658 were also collected. All these tissue samples were pre-  
659 pared for STEM-EDX observations of particle  
660 distribution.

#### 661 ICP-MS analysis of titanium

662 Placenta biopsies, foetal flow through collected during  
663 perfusion and meconium were analysed for Ti con-  
664 centration with a Thermo Element XR mass spec-  
665 trometer (ThermoFischer, Bremen, Germany)  
666 operated in high resolution mode. Samples were  
667 injected with a Seaspray nebulizer in self-aspiration  
668 (Glass expansion, Melbourne, Australia) and a quartz  
669 double-Scott Peltier-cooled spray chamber. Measure-  
670 ments were performed on isotopes  $^{47}\text{Ti}$ ,  $^{48}\text{Ti}$  and

$^{49}\text{Ti}$ , and Ti concentrations were calculated based on 671  
the average signals of the three isotopes. The instru- 672  
ment was tuned daily according to the manufacturer's 673  
recommendations, and the Ti spectra were confirmed 674  
to be free of interference, particularly calcium inter- 675  
ference, and its effect on  $^{48}\text{Ti}$  was correctly resolved. 676  
For foetal exudate, due to the high Ca content (0.49 677  
mM) of the Earle's medium used for perfusion, only 678  
signals on  $^{47}\text{Ti}$  and  $^{49}\text{Ti}$  were selected for 679  
calculations. 680

681 Prior to analysis, placental tissue samples were dry- 682  
ashed at  $700^\circ\text{C}$  in a furnace to burn the organic content 683  
without damaging the mineral particles. For foetal exu- 684  
date, each 10-min pool (50 mL) collected during placental 685  
perfusion (90 min) was evaporated at  $120^\circ\text{C}$  to near dry- 686  
ness to preconcentrate the sample. Placental tissue ashes 687  
and preconcentrated perfusates were digested by the 688  
addition of 0.5 mL of HF (40% HF, Suprapur<sup>®</sup>, Merck) 689  
and 10 mL of  $\text{HNO}_3$  (65%  $\text{HNO}_3$ , Suprapur<sup>®</sup>, Merck), 690  
evaporated at  $120^\circ\text{C}$ , and suspended in ultrapure water 691  
to a final volume of 50 mL. The recovery rates of these 692  
procedures were assessed by spiking samples with E171, 693  
and yielded 104% for the placental tissues and 85% for 694  
the exudates. Digestion blanks and control perfusates 695  
(no E171 addition) were used to correct the Ti concen- 696  
trations from blank contributions. 697

698 For meconium, approximately 0.5 mg was sampled 699  
and digested in 0.5 mL of HF and 10 mL of  $\text{HNO}_3$  and 700  
maintained at room temperature (RT) for 2 days before 701  
evaporation at  $60^\circ\text{C}$ . These steps were repeated once or 702  
twice until complete digestion. The samples were then 703  
diluted in 15 mL of ultrapure water and subsequently di- 704  
luted in 2%  $\text{HNO}_3$  for analysis. The recovery rates of this 705  
procedure were assessed against NIST 1566b and yielded 706  
 $99.9 \pm 10.2\%$  on average ( $n = 2$ , 1 S.D.). 707

708 The LOD was calculated as 3 times the standard devi- 709  
ation in the results of a blank sample and the LOQ as 10  
times the standard deviation, and the results are shown  
in mg/kg or ng/mL for each sample.

#### 710 Particle detection in the perfusion medium by confocal 711 microscopy

712 For each perfused placenta, a 35  $\mu\text{L}$  volume droplet of  
713 the foetal exudate collected every 5 min from  $t_0$  to  
714  $t_{90}$  min of perfusion was placed on 8-well microscopy  
715 slides, dried, and mounted in Mowiol medium (gly-  
716 cerol 240 g/L, DABCO 25 g/L, Mowiol 4-88 96 g/L,  
717 Tris-HCl 15 g/L) within 24 h after the collect. The  
718 slides were then examined under a confocal micros-  
719 cope (Leica SP8) at 488/BP 488-494 nm to detect  
720 light scattering (i.e., laser-diffracting)  $\text{TiO}_2$  particles  
721 appearing as green fluorescence and at 514/BP 560-  
722 660 nm to monitor autofluorescence in the sample, as  
723 previously described [7, 8]. Three fields per well were

724 examined, and laser-diffracting (particle) spots were  
725 counted using a 63X objective and a magnification  
726 factor of 1 pixel to 50 nm. Particles counted in the  
727 microscopic fields corresponding to exudate samples  
728 from the equilibrium period (from 10 to 30 min) and  
729 over the whole experiment with a control placenta  
730 perfused with PM alone were considered the back-  
731 ground level. To obtain a transfer profile to the foetal  
732 circuit of TiO<sub>2</sub> particles during 1 h after E171  
733 addition in the maternal reservoir, we calculated the  
734 background particle level as an average number of  
735 particles per observed field, and the value was sub-  
736 tracted from each corresponding value in all placentae  
737 perfused with the E171 suspension.

### 738 Preparation of foetal exudate samples for SEM-EDX 739 analysis

740 To characterize the particles crossing the human pla-  
741 centa, we selected pooled samples from foetal exudate  
742 (50 mL) corresponding to the 20–30 min of perfusion  
743 after E171 addition in the maternal reservoir based on  
744 the particle transfer profile by confocal imaging. Samples  
745 were lyophilized to concentrate the particles, and 5 g of  
746 powder was suspended in 1 mL of HCl to dissolve or-  
747 ganic compounds, sonicated (20 min, 75 W), and centri-  
748 fugal (10 min, 9503 g) and the supernatant was  
749 eliminated. The sample was then washed 5 times as fol-  
750 lows: addition of 1 mL of HCl, sonication (1 min, 150  
751 W), centrifugation (10 min, 9503 g) and elimination of  
752 the supernatant. The preparation was suspended in 1 mL  
753 of HCl, and then, a 7.5 µL droplet was deposited onto a  
754 silica wafer by spin-coating according to a method devel-  
755 oped by the LNE to perform NP dimensional metrology  
756 in complex matrices [69, 70]. Briefly, for good dispersion  
757 of the NPs on the silicon substrate while the solvent  
758 evaporated, the droplet was spread over the surface of  
759 the silica wafer using a low spin speed (1000 rpm, 5  
760 min), and then dried rapidly for 10 s at a fast spin speed  
761 (8000 rpm). The samples were stored at RT under a con-  
762 trolled atmosphere until observation.

763 SEM imaging was performed using a Zeiss Ultra-Plus  
764 field emission (FE) microscope equipped with a Gemini  
765 optical column. Images were obtained through second-  
766 ary electrons collected by an InLens detector at a voltage  
767 of 3 kV and with a working distance equal to 3 mm. In  
768 these working conditions, the provider claimed the reso-  
769 lution of the microscope was 1.7 nm. An EDX detector  
770 (Princeton Gamma-Tech Instruments, Princeton, USA)  
771 was installed in the SEM chamber for a qualitative elem-  
772 ental analysis of the observed particles. The size distribu-  
773 tion of the TiO<sub>2</sub> particles observed with SEM-EDX was  
774 assessed in a semiquantitative way with ImageJ software  
775 (NIH, USA), in PM containing 15 µg/mL of E171 and in  
776 foetal exudate from 2 placentae.

### Tissue preparation for TEM

777 Samples from 2 placentae and 2 meconium were fixed in  
778 2% paraformaldehyde-2.5% glutaraldehyde in 0.1 M  
779 cacodylate buffer (pH 7.4) for 1 h at 4 °C. For placentae,  
780 tissue blocks of 2.5 mm length were excised and  
781 immersed in the same fixative overnight at 4 °C. After  
782 several rinses in cacodylate buffer, the samples were in  
783 1% OsO<sub>4</sub> (Osmium (VIII) oxide) for 1 h at 4 °C and rap-  
784 idly rinsed again. Dehydration was carried out at 4 °C  
785 using a graded series of ethanol and acetone. The sec-  
786 tions were impregnated with low viscosity epoxy resin  
787 (EMS) under a vacuum and polymerized at 60 °C for  
788 48–72 h. Ultrathin sections (50–60 nm, ultra-cut UCT,  
789 Leica) were collected on gold–600 mesh grids and  
790 stained for 7 min with 0.5% uranyl acetate in methanol  
791 solution before TEM observations. The same protocol  
792 was used for meconium samples, except that osmium  
793 post-fixation and uranyl staining were not performed.  
794

### Scanning (S)TEM-EDX analysis, elemental mapping and particle size measurement

795 TEM-EDX analysis was performed on a JEM 2010  
796 (JEOL, Tokyo, Japan) operating at 120 kV and equipped  
797 with a LaB<sub>6</sub> cathode and two CCD cameras (Orius 1000  
798 and ES500W) driven by Digital Micrograph software  
799 (Gatan-Ametek, Pleasanton, United States). EDX-  
800 analysis was performed with a Silicon-drifted Detector  
801 (SDD) (Resolution: 125 eV Mn<sub>K</sub>) (Oxford-Instruments,  
802 Abington, Oxfordshire, England). Elemental mapping  
803 was performed on JEM-ARM200F HR-TEM (JEOL,  
804 Tokyo, Japan) with analytical configurations. Elemental  
805 maps were acquired at 80 kV in STEM mode with an 8C  
806 probe size, a camera length of 8 cm, and a 50 µm con-  
807 denser aperture with an SDD detector XMax TLE (Reso-  
808 lution: 127 eV Mn<sub>K</sub> 0.7 sr; Oxford-Instruments, Abington,  
809 England). Size measurement was determined from  
810 bright-field TEM images by using the image processing  
811 open-source software ImageJ (NIH, United States).  
812  
813

### Data analysis

814 The data are presented as the mean ± SD for determi-  
815 nation of the TiO<sub>2</sub> particle diameter in an E171 water sus-  
816 pension and for the Ti dosage in the placentae and the  
817 meconium (Table 1, Table 2) or as the mean ± SEM for  
818 particle counts and size measurements in the placenta  
819 and meconium TEM sections and in the foetal exudate  
820 (Figs. 3, and 5).  
821

### Supplementary information

822 Supplementary information accompanies this paper at <https://doi.org/10.1186/s12989-020-00381-z>.  
823  
824

Additional file 1 Table S1. ICP-MS analysis of Ti content in foetal exudate collected during control or E171 perfusion. Ti content of foetal

826  
827  
828

exudates from 6 independent E171 perfusion experiments (15 µg/mL) and 1 control perfusion. Samples were collected by time fraction of 10- or (\*15)-min during perfusion (first 30 min of 1 h for E5 and E6, total 60 min for E1, E2, E3, E4, and E7). All concentrations are corrected for total blank signals. LOD = 0.23 ng/mL. Typical relative measurement uncertainty was 5% (k = 1). **Fig. S1.** Basal particulate content in term human placenta. (A and B) Representative TEM-Bright Field micrographs showing particulate matter in the placental tissues. Elemental characterization was determined by TEM-EDX analysis. In addition to Carbon and Oxygen, the following elements were found: ⊙: Tin, Iron, Silicon; ⊚: Silicon; ⊛: Tin, Zinc, Iron, Manganese, Phosphorus, Silicon; ⊜: Silicon; ⊝: Iron, Aluminium, Silicon; ⊞: Silicon, Aluminium; ⊟: Silicon, Aluminium. (C) EDX-Blank spectrum of biological matrix: elements in deconvolution are Uranium (U), Osmium (Os), Gold (Au), Copper (Cu), Chromium (Cr) coming from grids, sample preparation and staining of TEM pieces. **Fig. S2.** Particle diameter distribution in term human placenta. Size measurement of particles recovered per field micrograph on ultrafine sections from 2 placentae collected at term of pregnancy. Dashed line represents the 100 nm limit. **Fig. S3.** Basal particulate content in human meconium. (A to C) TEM-Bright Field micrographs of meconium ultrafine sections showing particles in meconium, and combined TEM-EDX analysis for elemental characterization; ⊙: Iron (Fe), Silicon (Si), Magnesium (Mg), Calcium (Ca), Aluminium (Al); ⊚: Titanium (Ti), Aluminium (Al), Silicon (Si). Elements in deconvolution are Gold (Au), Copper (Cu), Chromium (Cr) coming from grids, sample preparation of TEM pieces. **Fig. S4.** Antipyrine rate transfer depending on the placental origin. Foeto-maternal rate transfer of antipyrine during ex vivo perfusions of placentae collected after vaginal delivery (n = 5) or caesarean section (n = 6). Note that there is no difference in basal permeability depending on the mode of delivery. Data are presented as mean ± SD. **Fig. S5.** Confocal imaging of laser-diffracting particles in perfusion medium with E171, foetal exudate and perfused placenta. (A) Laser-diffracting particles in the E171-containing PM added to maternal side. Scale bar = 50 µm. (B) Foetal exudate collected between 30 and 35 min of E171 perfusion. White arrows indicate laser-diffracting particles. Scale bars = 50 µm. (C) Tissue section of perfused placenta showing laser-diffracting particles spread in the intervillous spaces (ivs) of the maternal side close to the syncytiotrophoblast (sct). White arrows indicate foetal vessels. Scale bar = 100 µm. **Fig. S6.** Complementary EDX analysis of foetal exudates. Purified samples of particles recovered in foetal exudates and showing (A) aluminium (Al) and (B) iron (Fe) elements associated or not with titanium (Ti). Corresponding SEM micrographs of purified particles in upper right panels; Si signal from SEM wafer. **Fig. S7.** Method for size measurement of TiO<sub>2</sub> particles in the foetal exudate. (A) and (B) TiO<sub>2</sub> particles were identified by an EDX detector coupled to SEM chamber for Ti (green) and O (red) element analysis (upper right panels in A and B), and observed as agglomerates (A) or as isolated particles or small aggregates trapped into the matrix of dried PM after sample preparation, i.e., resulting from the sample deposition onto silicate wafer by spin-coating and evaporation of the solvent [62]. Only the diameters of particles showing Ti + O colocalization (yellow) were measured, here for some particles as examples. Scale bar = 200 nm. **Fig. S8.** Size measurement of TiO<sub>2</sub> particles in two representative E171-perfused placentae. (A) TEM image reconstruction showing tissue architecture across a placental villus along the materno-foetal axis, i.e., the syncytiotrophoblast microvilli and syncytiotrophoblast cells, the cytotrophoblast cells, then the chorionic mesenchyme composed of the basal lamina supporting trophoblast tissue, and the endothelial cells surrounding foetal capillaries. (B and C) Size distribution of TiO<sub>2</sub> (EDX-characterized) particles into perfused placenta, (B) trapped into microvilli of the syncytiotrophoblast on the maternal side, and (C) in deeper area until close to foetal vessels. (D) Representative TEM images of perfused TiO<sub>2</sub> particles (arrowheads) recovered in the intervillous spaces (ivs) close to the syncytiotrophoblast microvilli (D1) and into the placental chorionic mesenchyme surrounding foetal capillaries (D2).

#### 894 Acknowledgements

895 The authors wish to thank Sebastien Cambier (Luxembourg Institute of  
896 Science and Technology) for preliminary ICP-MS measurements. Nora Lam-  
897 beng and Caroline Oster (LNE) are also thanks for their help during SEM-EDX  
898 and ICP-MS analysis, respectively. All the nurses of the Toulouse University

Hospital who participated to the placentae collection, and Clemence Moiron 899  
and Dr. Laurent Petit (Clinique Sainte Thérèse, Paris) for their interest in this 900  
project. 901

#### 902 Authors' contributions

903 A.G., M.M., C.Co., V. G, K.C., C.V., F.de la F., N.P.-H., B.L. and E.H. designed the  
904 study; E.G., M.M., A.de P., V.B., K.C., N.B. and K.A.-P. contributed to sample  
905 collection; E.G., M.M., F.G., M.L., A.C. and A.G. conducted the perfusion  
906 experiments; A.G., C.Ca., L.D., L.C., and N.F. performed TEM, SEM-EDX and  
907 (S)TEM-EDX analysis; A.G. and J.N. performed ICP-MS measurements; M.L. per-  
908 formed antipyrine dosage; A.G., E.G., C.Ca., L.D., J.N., L.C., F.G., M.L., C.Co., V. G,  
909 V. B, K.C., K.A.-P., C.V., P.F., N.F., N.P.-H., B.L. and E.H. analyzed the data; A.G.,  
910 L.D., J.N., L.C., V. G, K.A.-P., F.de la F., N.P.-H., B.L. and E.H. wrote the paper. All  
911 author(s) read and approved the final manuscript.

#### 912 Funding

913 The study was supported by INRAE (Institut national de recherche pour  
914 l'agriculture, l'alimentation et l'environnement) and The Gerard Cazanave's  
915 Research Association. Adèle Guillard has fellowship from the French Ministry  
916 of Higher Education, Research and Innovation.

#### 917 Availability of data and materials

918 All relevant data are included in the manuscript and supporting information,  
919 and available from the authors upon request.

#### 920 Ethics approval and consent to participate

921 The collect of human placenta and use for ex vivo perfusion was performed  
922 following the principles of the Declaration of Helsinki and written informed  
923 consent was given by the mothers before delivery. The study was approved  
924 by the local ethics committee (DC-2013-1950). Meconium samples were  
925 obtained under an internal agreement of the scientific committee or from  
926 volunteer parents, and informed signed consents were obtained from all  
927 parents.

#### 928 Consent for publication

929 All authors read and approved the final manuscript.

#### 930 Competing interests

931 Authors declare that they have no competing interests.

#### 932 Author details

933 <sup>1</sup>Toxalim UMR1331 (Research Centre in Food Toxicology), Toulouse  
934 University, INRAE, ENVT, INP-Purpan, UPS, Toulouse, France. <sup>2</sup>Department of  
935 materials, LNE, Trappes, France. <sup>3</sup>Department for biomedical and inorganic  
936 chemistry, LNE, Paris, France. <sup>4</sup>Group Physic of Materials, GPM-UMR6634,  
937 CNRS, Rouen University, Rouen, France. <sup>5</sup>Department of Obstetrics and  
938 Gynecology, Paule de Viguier Hospital, CHU Toulouse, Toulouse, France. <sup>6</sup>IN-  
939 THERES, UMR 1436 Toulouse University, INRAE, ENVT, Toulouse, France.  
940 <sup>7</sup>Péritox UMR-I 01 (Perinatal and Toxic Risk), Jules Verne University, Amiens,  
941 France. <sup>8</sup>Université Paris Saclay, CEA, INRAE, Paris, France. <sup>9</sup>Département  
942 Médicaments et Technologies pour la Santé (DMTS), SPI, 91191  
943 Gif-sur-Yvette, France. <sup>10</sup>UMR 1027 INSERM, Team SPHERE, Toulouse III  
944 University, Toulouse, France.

945 Received: 6 May 2020 Accepted: 14 September 2020

#### 947 References

- 948 Skocaj M, Filipic M, Petkovic J, Novak S. Titanium dioxide in our everyday  
949 life; is it safe? *Radiol Oncol.* 2011;45:227–47.
- 950 Weir A, Westerhoff P, Fabricius L, Hristovski K, von Goetz N. Titanium dioxide  
951 nanoparticles in food and personal care products. *Environ Sci Technol.*  
952 2012;46:2242–50.
- 953 Shakeel M, Jabeen F, Shabbir S, Asghar MS, Khan MS, Chaudhry AS. Toxicity  
954 of Nano-titanium dioxide (TiO<sub>2</sub>-NP) through various routes of exposure: a  
955 review. *Biol Trace Elem Res.* 2016;172:1–36.
- 956 Böckmann J, Lahl H, Eckert T, Unterhalt B. Blood levels of titanium before  
957 and after oral administration of titanium dioxide. *Pharmazie.* 2000;55:140–3.
- 958 Pele LC, Thoree V, Bruggaber SF, Koller D, Thompson RP, Lomer MC, et al.  
959 Pharmaceutical/food grade titanium dioxide particles are absorbed into the  
960 bloodstream of human volunteers. *Part Fibre Toxicol.* 2015;12:26.

- 961 6. Jones K, Morton J, Smith I, Jurkschat K, Harding A-H, Evans G. Human  
962 *in vivo* and *in vitro* studies on gastrointestinal absorption of titanium  
963 dioxide nanoparticles. *Toxicol Lett.* 2015;233:95–101.
- 964 7. Bettini S, Boutet-Robinet E, Cartier C, Coméra C, Gaultier E, Dupuy J, et al.  
965 Food-grade TiO<sub>2</sub> impairs intestinal and systemic immune homeostasis,  
966 initiates preneoplastic lesions and promotes aberrant crypt development in  
967 the rat colon. *Sci Rep.* 2017;7:40373.
- 968 8. Coméra C, Cartier C, Gaultier E, Catrice O, Panouille Q, El Hamdi S,  
969 et al. Jejunal villus absorption and paracellular tight junction  
970 permeability are major routes for early intestinal uptake of food-grade  
971 TiO<sub>2</sub> particles: an *in vivo* and *ex vivo* study in mice. *Part Fibre Toxicol.*  
972 2020;17:26.
- 973 9. Heringa MB, Peters RJB, Bley RLAW, van der Lee MK, Tromp PC, van  
974 Kesteren PCE, et al. Detection of titanium particles in human liver and  
975 spleen and possible health implications. *Part Fibre Toxicol.* 2018;15:15.
- 976 10. Abbasi-Oshaghi E, Mirzaei F, Pourjafar M. NLRP3 inflammasome, oxidative  
977 stress, and apoptosis induced in the intestine and liver of rats treated with  
978 titanium dioxide nanoparticles: *in vivo* and *in vitro* study. *Int J*  
979 *Nanomedicine.* 2019;14:1919–36.
- 980 11. Zhang L, Xie X, Zhou Y, Yu D, Deng Y, Ouyang J, et al. Gestational exposure  
981 to titanium dioxide nanoparticles impairs the placental transfer through  
982 dysregulation of vascularization, proliferation and apoptosis in mice. *IJN.*  
983 2018;13:777–89.
- 984 12. Chakrabarti S, Goyary D, Karmakar S, Chattopadhyay P. Exploration of  
985 cytotoxic and genotoxic endpoints following sub-chronic oral exposure to  
986 titanium dioxide nanoparticles. *Toxicol Ind Health.* 2019;35:577–92.
- 987 13. Dhupal M, Oh J-M, Tripathy DR, Kim S-K, Koh SB, Park K-S. Immunotoxicity  
988 of titanium dioxide nanoparticles via simultaneous induction of apoptosis  
989 and multiple toll-like receptors signaling through ROS-dependent SAPK/JNK  
990 and p38 MAPK activation. *Int J Nanomedicine.* 2018;13:6735–50.
- 991 14. Suzuki T, Miura N, Hojo R, Yanagiba Y, Suda M, Hasegawa T, et al.  
992 Genotoxicity assessment of titanium dioxide nanoparticle accumulation of  
993 90 days in the liver of gpt delta transgenic mice. *Genes Environ.* 2020;42:7.
- 994 15. EFSA Panel on Food Additives and Nutrient Sources added to Food (ANS).  
995 Re-evaluation of titanium dioxide (E171) as a food additive. *EFSA Journal.*  
996 2016;14.
- 997 16. Dorier M, Béal D, Marie-Desvergne C, Dubosson M, Barreau F, Houdeau E,  
998 et al. Continuous *in vitro* exposure of intestinal epithelial cells to E171 food  
999 additive causes oxidative stress, inducing oxidation of DNA bases but no  
1000 endoplasmic reticulum stress. *Nanotoxicology.* 2017;1–11.
- 1001 17. Yamashita K, Yoshioka Y, Higashisaka K, Mimura K, Morishita Y, Nozaki M,  
1002 et al. Silica and titanium dioxide nanoparticles cause pregnancy  
1003 complications in mice. *Nature Nanotech.* 2011;6:321–8.
- 1004 18. Umezawa. Effect of Fetal Exposure to Titanium Dioxide Nanoparticle on  
1005 Brain Development - Brain Region Information. *J Toxicol Sci.* 37:6.
- 1006 19. Mölsä M, Heikkinen T, Hakkola J, Hakala K, Wallerman O, Wadelius M,  
1007 et al. Functional role of P-glycoprotein in the human blood-placental  
1008 barrier. *Clin Pharmacol Therapeutics.* John Wiley & Sons Ltd. 2005;78:  
1009 123–31.
- 1010 20. Hemauer SJ, Patrikeeva SL, Wang X, Abdelrahman DR, Hankins GDV, Ahmed  
1011 MS, et al. Role of transporter-mediated efflux in the placental biodisposition  
1012 of bupropion and its metabolite, OH-bupropion. *Biochem Pharmacol.* 2010;  
1013 80:1080–6.
- 1014 21. Delorme-Axford E, Bayer A, Sadovsky Y, Coyne CB. Autophagy as a  
1015 mechanism of antiviral defense at the maternal–fetal interface. *Autophagy*  
1016 Taylor Francis. 2013;9:2173–4.
- 1017 22. Rollerova E, Tulinska J, Liskova A, Kuricova M, Kovriznych J, Mlynarcikova A,  
1018 et al. Titanium Dioxide Nanoparticles. 2015;49:97–112.
- 1019 23. Mohammadpour A, Fazel A, Haghiri H, Motejaded F, Rafatpanah H, Zabihi H,  
1020 et al. Maternal exposure to titanium dioxide nanoparticles during  
1021 pregnancy; impaired memory and decreased hippocampal cell proliferation  
1022 in rat offspring. *Environ Toxicol Pharmacol.* 2014;37:617–25.
- 1023 24. Ebrahimzadeh Bideskan A, Mohammadpour A, Fazel A, Haghiri H,  
1024 Rafatpanah H, Hosseini M, et al. Maternal exposure to titanium dioxide  
1025 nanoparticles during pregnancy and lactation alters offspring hippocampal  
1026 mRNA BAX and Bcl-2 levels, induces apoptosis and decreases neurogenesis.  
1027 *Exp Toxicol Pathol.* 2017;69:329–37.
- 1028 25. Gao X, Yin S, Tang M, Chen J, Yang Z, Zhang W, et al. Effects of  
1029 developmental exposure to TiO<sub>2</sub> nanoparticles on synaptic plasticity in  
1030 hippocampal dentate Gyrus area: an *in vivo* study in anesthetized rats. *Biol*  
1031 *Trace Elem Res.* 2011;143:1616–28.
26. Takeda K, Suzuki K, Ishihara A, Kubo-Irie M, Fujimoto R, Tabata M, et al. 1032  
Nanoparticles transferred from pregnant mice to their offspring can 1033  
damage the genital and cranial nerve systems. *J Health Sci.* 2009;55:95–102. 1034
27. Schmidt A, Morales-Prieto DM, Pastuschek J, Fröhlich K, Markert UR. Only 1035  
humans have human placentas: molecular differences between mice and 1036  
humans. *J Reprod Immunol.* 2015;108:65–71. 1037
28. Enders AC, Blankenship TN. Comparative placental structure. *Adv Drug Deliv* 1038  
*Rev.* 1999;38:3–15. 1039
29. Li X, Li A, Zhang W, Liu X, Liang Y, Yao X, et al. A pilot study of mothers and 1040  
infants reveals fetal sex differences in the placental transfer efficiency of 1041  
heavy metals. *Ecotoxicol Environ Saf.* 2019;186:109755. 1042
30. Woźniak MK, Jaszczak E, Wiergowski M, Polkowska Ż, Namieśnik J, Biziuk M. 1043  
Meconium analysis as a promising diagnostic tool for monitoring fetal 1044  
exposure to toxic substances: recent trends and perspectives. *TrAC Trends* 1045  
*Anal Chem.* 2018;109:124–41. 1046
31. Wick P, Malek A, Manser P, Meili D, Maeder-Althaus X, Diener L, et al. Barrier 1047  
capacity of human placenta for Nanosized materials. *Environ Health* 1048  
*Perspect.* 2010;118:432–6. 1049
32. Grafmueller S, Manser P, Diener L, Diener P-A, Maeder-Althaus X, Maurizi L, 1050  
et al. Bidirectional transfer study of polystyrene nanoparticles across the 1051  
placental barrier in an *ex Vivo* human placental perfusion model. *Environ* 1052  
*Health Perspect.* 2015;123:1280–6. 1053
33. Poulsen MS, Mose T, Maroun LL, Mathiesen L, Knudsen LE, Rytting E. 1054  
Kinetics of silica nanoparticles in the human placenta. *Nanotoxicology.* 2015; 1055  
9:79–86. 1056
34. Muoth C, Wichser A, Monopoli M, Correia M, Ehrlich N, Loeschner K, et al. A 1057  
3D co-culture microtissue model of the human placenta for nanotoxicity 1058  
assessment. *Nanoscale.* 2016;8:17322–32. 1059
35. Aengenheister L, Dugershaw BB, Manser P, Wichser A, Schoenenberger R, Wick 1060  
P, et al. Investigating the accumulation and translocation of titanium dioxide 1061  
nanoparticles with different surface modifications in static and dynamic 1062  
human placental transfer models. *Eur J Pharm Biopharm.* 2019;142:488–97. 1063
36. Iwai-Shimada M, Nakayama SF, Isobe T, Kobayashi Y, Suzuki G, Nomura K. 1064  
Investigation of the Effects of Exposure to Chemical Substances on Child 1065  
Health. *Nihon Eiseigaku Zasshi.* 2019;74. 1066
37. Gaffet E, Marano F, Ferrari L, Flahaut E, Jouzel J-N, Madec L, et al. Bilan des 1067  
connaissances relatives aux effets des nanoparticules de TiO<sub>2</sub> sur la santé 1068  
humaine ; caractérisation de l'exposition des populations et mesures de 1069  
gestion. 2018 Available from: [https://www.researchgate.net/publication/326007817\\_Bilan\\_des\\_connaissances\\_relatives\\_aux\\_effets\\_des\\_nanoparticules\\_de\\_TiO2\\_sur\\_la\\_sante\\_humaine\\_caracterisation\\_de\\_l%27exposition\\_des\\_populations\\_et\\_mesures\\_de\\_gestion](https://www.researchgate.net/publication/326007817_Bilan_des_connaissances_relatives_aux_effets_des_nanoparticules_de_TiO2_sur_la_sante_humaine_caracterisation_de_l%27exposition_des_populations_et_mesures_de_gestion). 1070  
1071
38. Li A, Zhuang T, Shi J, Liang Y, Song M. Heavy metals in maternal and cord 1072  
blood in Beijing and their efficiency of placental transfer. *J Environ Sci.* 2019; 1073  
80:99–106. 1074
39. Raia-Barjat T, Prieux C, Leclerc L, Sarry G, Grimal L, Chaleur C, et al. 1075  
Elemental fingerprint of human amniotic fluids and relationship with 1076  
potential sources of maternal exposure. *J Trace Elem Med Biol.* 2020;60:  
1077 126477. 1078
40. Lu PJ, Fang SW, Cheng WL, Huang SC, Huang MC, Cheng HF. 1079  
Characterization of titanium dioxide and zinc oxide nanoparticles in 1080  
sunscreen powder by comparing different measurement methods. *J Food* 1081  
*Drug Anal.* 2018;26:1192–200. 1082
41. Lewicka ZA, Benedetto AF, Benoit DN, Yu WW, Fortner JD, Colvin VL. The 1083  
structure, composition, and dimensions of TiO<sub>2</sub> and ZnO nanomaterials in 1084  
commercial sunscreens. *J Nanopart Res.* 2011;13:3607. 1085
42. Saber AT, Jacobsen NR, Mortensen A, Szarek J, Jackson P, Madsen AM, et al. 1086  
Nanotitanium dioxide toxicity in mouse lung is reduced in sanding dust 1087  
from paint. *Part Fibre Toxicol.* 2012;9:4. 1088
43. Mikkelsen L, Jensen KA, Koponen IK, Saber AT, Wallin H, Loft S, et al. 1089  
Cytotoxicity, oxidative stress and expression of adhesion molecules in 1090  
human umbilical vein endothelial cells exposed to dust from paints with or 1091  
without nanoparticles. *Nanotoxicology.* 2013;7:117–34. 1092
44. Saber AT, Mortensen A, Szarek J, Jacobsen NR, Levin M, Koponen IK, et al. 1093  
Toxicity of pristine and paint-embedded TiO<sub>2</sub> nanomaterials. *Hum Exp* 1094  
*Toxicol.* 2019;38:11–24. 1095
45. Filippini T, Tancredi S, Malagoli C, Cilloni S, Malavolti M, Violi F, et al. 1096  
Aluminum and tin: food contamination and dietary intake in an Italian 1097  
population. *J Trace Elem Med Biol.* 2019;52:293–301. 1098
46. Grigoratos T, Martini G. Brake wear particle emissions: a review. *Environ Sci* 1099  
*Pollut Res Int.* 2015;22:2491–504. 1100  
1101  
1102

- 1103 47. Martin J, Bello D, Bunker K, Shafer M, Christiani D, Woskie S, et al. Occupational exposure to nanoparticles at commercial photocopy centers. *J Hazard Mater*. 2015;298:351–60.
- 1104
- 1105
- Q8 1106 48. Gonet T, Maher BA. Airborne, vehicle-derived Fe-bearing nanoparticles in the urban environment: a review. *Environ Sci Technol*. 2019;53:9970–91..
- 1107
- 1108 49. Iwai-Shimada M, Kameo S, Nakai K, Yaginuma-Sakurai K, Tatsuta N, Kurokawa N, et al. Exposure profile of mercury, lead, cadmium, arsenic, antimony, copper, selenium and zinc in maternal blood, cord blood and placenta: the Tohoku study of child development in Japan. *Environ Health Prev Med*. 2019;24:35.
- 1109
- 1110
- 1111
- 1112
- 1113 50. Berton T, Mayhoub F, Chardon K, Duca R-C, Lestremou F, Bach V, et al. Development of an analytical strategy based on LC-MS/MS for the measurement of different classes of pesticides and their metabolites in meconium: application and characterisation of foetal exposure in France. *Environ Res*. 2014;132:311–20..
- 1114
- 1115
- 1116
- Q9 1117
- 1118 51. Beall MH, van den Wijngaard JPHM, van Gemert MJC, Ross MG. Amniotic fluid water dynamics. *Placenta*. 2007;28:816–23.
- 1119
- 1120 52. Pietrouisti A, Vecchione L, Malvindi MA, Aru C, Massimiani M, Camaioni A, et al. Relevance to investigate different stages of pregnancy to highlight toxic effects of nanoparticles: the example of silica. *Toxicol Appl Pharmacol*. 2018;342:60–8.
- 1121
- 1122
- 1123
- 1124 53. Food Safety Commission of Japan. Aluminium Ammonium Sulfate and Aluminium Potassium Sulfate (Food Additives). *Food Saf (Tokyo)*. 2019;7:79–82.
- 1125
- 1126
- 1127 54. Winkler HC, Suter M, Naegeli H. Critical review of the safety assessment of nano-structured silica additives in food. *J Nanobiotechnol*. 2016;14:44.
- 1128
- 1129 55. Etwel F, Hutson JR, Madadi P, Gareri J, Koren G. Fetal and perinatal exposure to drugs and chemicals: novel biomarkers of risk. *Annu Rev Pharmacol Toxicol*. 2014;54:295–315.
- 1130
- 1131
- 1132 56. Heringa MB, Geraets L, van Eijkeren JCH, Vandebriel RJ, de Jong WH, Oomen AG. Risk assessment of titanium dioxide nanoparticles via oral exposure, including toxicokinetic considerations. *Nanotoxicology*. 2016;10:1515–25.
- 1133
- 1134
- 1135
- 1136 57. D'Errico JN, Doherty C, Fournier SB, Renkel N, Kallontzi S, Goedken M, et al. Identification and quantification of gold engineered nanomaterials and impaired fluid transfer across the rat placenta via ex vivo perfusion. *Biomed Pharmacother*. 2019;117:109148.
- 1137
- 1138
- 1139
- 1140 58. Semmler-Behnke M, Lipka J, Wenk A, Hirn S, Schäffler M, Tian F, et al. Size dependent translocation and fetal accumulation of gold nanoparticles from maternal blood in the rat. *Part Fibre Toxicol*. 2014;11:33.
- 1141
- 1142
- 1143 59. Buerki-Thumherr T, von Ursula M, Wick P. Knocking at the door of the unborn child: engineered nanoparticles at the human placental barrier. *Swiss Med Wkly [Internet]*. 2012; doi: <https://doi.org/10.4414/smw.2012.13559>.
- 1144
- 1145
- 1146
- 1147 60. Radziwill-Bienkowska JM, Talbot P, Kamphuis JBJ, Robert V, Cartier C, Fourquaux I, et al. Toxicity of food-grade TiO<sub>2</sub> to commensal intestinal and transient food-borne Bacteria: new insights using Nano-SIMS and synchrotron UV fluorescence imaging. *Front Microbiol*. 2018;9:794..
- 1148
- 1149
- Q10 1150
- 1151 61. Talbot P, Radziwill-Bienkowska JM, Kamphuis JBJ, Steenkeste K, Bettini S, Robert V, et al. Food-grade TiO<sub>2</sub> is trapped by intestinal mucus in vitro but does not impair mucin O-glycosylation and short-chain fatty acid synthesis in vivo: implications for gut barrier protection. *J Nanobiotechnol*. 2018;16:53.
- 1152
- 1153
- 1154
- 1155
- 1156 62. Li J, Yang S, Lei R, Gu W, Qin Y, Ma S, et al. Oral administration of rutile and anatase TiO<sub>2</sub> nanoparticles shifts mouse gut microbiota structure. *Nanoscale Royal Soc Chem*. 2018;10:7736–45.
- 1157
- 1158
- 1159 63. Chen H, Zhao R, Wang B, Cai C, Zheng L, Wang H, et al. The effects of orally administered Ag, TiO<sub>2</sub> and SiO<sub>2</sub> nanoparticles on gut microbiota composition and colitis induction in mice. *NanoImpact*. 2017;8:80–8.
- 1160
- 1161
- 1162 64. Lamas B, Martins Breyner N, Houdeau E. Impacts of foodborne inorganic nanoparticles on the gut microbiota-immune axis: potential consequences for host health. *Part Fibre Toxicol*. 2020;17:19.
- 1163
- 1164
- 1165 65. Zhang Y, Xu B, Yao M, Dong T, Mao Z, Hang B, et al. Titanium dioxide nanoparticles induce proteostasis disruption and autophagy in human trophoblast cells. *Chem Biol Interact*. 2018;296:124–33.
- 1166
- 1167
- 1168 66. Mao Z, Yao M, Li Y, Fu Z, Li S, Zhang L, et al. miR-96-5p and miR-101-3p as potential intervention targets to rescue TiO<sub>2</sub> NP-induced autophagy and migration impairment of human trophoblastic cells. *Biomater Sci*. 2018;6:3273–83.
- 1169
- 1170
- 1171
- 1172 67. Mao Z, Guan Y, Li T, Zhang L, Liu M, Xing B, et al. Up regulation of miR-96-5p is responsible for TiO<sub>2</sub> NPs induced invasion dysfunction of human trophoblastic cells via disturbing Ezrin mediated cytoskeletons arrangement. *Biomed Pharmacother*. 2019;117:109125.
- 1173
- 1174
68. Corbel T, Gayraud V, Puel S, Lacroix MZ, Berrebi A, Gil S, et al. Bidirectional placental transfer of Bisphenol a and its main metabolite, Bisphenol A-Glucuronide, in the isolated perfused human placenta. *Reprod Toxicol*. 2014;47:51–8.
- 1175
- 1176
- 1177
- 1178
- 1179
69. Delvallée A, Feltin N, Ducourtieux S, Trabelsi M, Hochepeid JF. Direct comparison of AFM and SEM measurements on the same set of nanoparticles. *Meas Sci Technol*. 2015;26:085601.
- 1180
- 1181
- 1182
70. Devoille L, Revel M, Batana C, Feltin N, Giambérini L, Châtel A, et al. Combined influence of oxygenation and salinity on aggregation kinetics of the silver reference nanomaterial NM-300K. *Environ Toxicol Chem*. 2018;37:1007–13.
- 1183
- 1184
- 1185
- 1186

## Publisher's Note

Springer Nature remains neutral with regard to jurisdictional claims in published maps and institutional affiliations.

1187  
1188  
1189

**Ready to submit your research? Choose BMC and benefit from:**

- fast, convenient online submission
- thorough peer review by experienced researchers in your field
- rapid publication on acceptance
- support for research data, including large and complex data types
- gold Open Access which fosters wider collaboration and increased citations
- maximum visibility for your research: over 100M website views per year

At BMC, research is always in progress.

Learn more [biomedcentral.com/submissions](https://biomedcentral.com/submissions)



# Author Query Form

---

**Journal: Particle and Fibre Toxicology**

**Title: Basal Ti level in the human placenta and meconium and evidence of a materno-foetal transfer of food-grade TiO<sub>2</sub> nanoparticles in an ex vivo placental perfusion model**

[Q1]

**Authors: A. Guillard, E. Gaultier, C. Cartier, L. Devoille, J. Noireaux, L. Chevalier, M. - Morin, F. Grandin, M. Z. Lacroix, C. Coméra, A. Cazanave, A. de Place, V. Gayrard, V. - Bach, K. Chardon, N. Bekhti, K. Adel-Patient, C. Vayssière, P. Fisicaro, N. Feltin, F. de la Farge, N. Picard-Hagen, B. Lamas, E. Houdeau**

**Article: 381**

Dear Authors,

During production of your paper, the following queries arose. Please respond to these by annotating your proofs with the necessary changes/additions. If you intend to annotate your proof electronically, please refer to the E-annotation guidelines. We recommend that you provide additional clarification of answers to queries by entering your answers on the query sheet, in addition to the text mark-up.

Query No.	Query	Remark
Q1	Author names: Please confirm if the author names are presented accurately (given names/initials, family name). Author 1: Given name: A. Family name: Guillard Author 2: Given name: E. Family name: Gaultier Author 3: Given name: C. Family name: Cartier Author 4: Given name: L. Family name: Devoille Author 5: Given name: J. Family name: Noireaux Author 6: Given name: L. Family name: Chevalier Author 7: Given name: M. Family name: Morin Author 8: Given name: F. Family name: Grandin Author 9: Given name: M.	

Query No.	Query	Remark
	<p>Given name: Z.  Family name: Lacroix  Author 10:  Given name: C.  Family name: Coméra  Author 11:  Given name: A.  Family name: Cazanave  Author 12:  Given name: A.  Particle: de  Family name: Place  Author 13:  Given name: V.  Family name: Gayrard  Author 14:  Given name: V.  Family name: Bach  Author 15:  Given name: K.  Family name: Chardon  Author 16:  Given name: N.  Family name: Bekhti  Author 17:  Given name: K.  Family name: Adel-Patient  Author 18:  Given name: C.  Family name: Vayssière  Author 19:  Given name: P.  Family name: Fisticaro  Author 20:  Given name: N.  Family name: Feltin  Author 21:  Given name: F.  Particle: de la  Family name: Farge  Author 22:  Given name: N.  Family name: Picard-Hagen  Author 23:  Given name: B.  Family name: Lamas  Author 24:  Given name: E.  Family name: Houdeau</p>	

Query No.	Query	Remark
Q2	As per standard instruction, city and country is required for affiliations; however, this information is missing in affiliation 8 Please check if the provided city and country is correct and amend if necessary.	
Q3	Affiliation (Université Paris Saclay, CEA, INRAE; Département Médicaments et Technologies pour la Santé (DMTS), SPI, 91191 Gif-sur-Yvette, France) was split into two different affiliations. Please check if appropriate and amend if necessary.	
Q4	Please check if the affiliations are presented correctly.	
Q5	Please check if the section headings are assigned to appropriate levels.	
Q6	Figures 1-2,5-6 small and poor quality texts. Please provide replacement of figure files. Otherwise, kindly confirm if we can retain the current presentation.	
Q7	As per standard instruction, the statement “All authors read and approved the final manuscript.” is required in the “Authors’ contributions” section. Please note that this was inserted at the end of the paragraph of the said section. Please check if appropriate.	
Q8	Citation details for reference [16] is incomplete. Please supply the "volume" of this reference. Otherwise, kindly advise us on how to proceed.	
Q9	Citation details for reference [18] is incomplete. Please supply the "pages" of this reference. Otherwise, kindly advise us on how to proceed.	
Q10	Citation details for references [15 and 36] are incomplete. Please supply the "pages" of this reference. Otherwise, kindly advise us on how to proceed.	